CALIFORNIA INSTITUTE OF TECHNOLOGY

EARTHQUAKE ENGINEERING RESEARCH LABORATORY

STRONG-MOTION EARTHQUAKE MEASUREMENT USING A DIGITAL ACCELEROGRAPH

BY

WILFRED D. IWAN, MICHAEL A. MOSER
AND CHIA-YEN PENG

REPORT NO. EERL 84-02

PASADENA, CALIFORNIA

APRIL 1984

Strong-Motion Earthquake Measurement Using a Digital Accelerograph

By Wilfred D. Iwan, Michael A. Moser, and Chia-Yen Peng

ABSTRACT

This paper presents results of a study of some of the characteristics of the Kinemetrics PDR-1 digital strong-motion accelerograph. The paper gives the results of laboratory tests of the background noise level of the instrument and compares these results with previously reported observations for optical instruments. The determination of displacement from acceleration data is discussed and results of laboratory tests are presented. Certain instrument anomalies are identified, data correction algorithms proposed, and examples given. The paper also presents the results of a comparison of earthquake records obtained from side-by-side digital and optical analog instruments. Finally, some results obtained from a recent Chinese earthquake are discussed.

INTRODUCTION

The development of reliable, digital strong-motion accelerographs is having a very significant impact on the measurement of strong ground motion. After analog amplification, and conversion to digital format, the digital instruments record the data on magnetic tape or a core memory in a computer-readable form, thus bypassing many of the steps of the analog-to-digital conversion process associated with optical analog accelerographs. Timing is generally quite accurate in these digital recorders, being of the order of one part in 10^7. In addition, digital instruments commonly have a pre-event memory so that the entire history of the motion is recorded along with the initial

state of the instrument. The resolution of the digital instruments is typically 66 dB (with 12 bits of digital data), and the dynamic range is increased by 36 dB through the use of an autoranging analog amplifier.

Because of their inherent advantages, the use of digital instruments should become very widespread throughout the world in the years to come. However, since these instruments have only recently been put into service, their characteristics are not well known. The purpose of this paper is to present results of a study of the recording characteristics of a typical strong-motion recorder/transducer instrument. The background noise level of the recorded data is compared with that of optical recorders. Integration of the recorded acceleration time history to obtain displacement is discussed and the results of laboratory tests presented. Certain instrument anomalies are identified and correction algorithms are proposed. Also presented is a comparison of side-by-side recorded results obtained from analog and digital instruments.

NOISE LEVEL OF DIGITAL INSTRUMENT

Considerable laboratory and field experience has been gained with optical strong-motion recorders. The limitations of these instruments are fairly well understood and substantial effort has been expended to maximize the data return from such instruments using various filtering and correction algorithms (Hudson, 1979). Noise is introduced into the optical recording from a number of sources including transducer drift, recording medium lateral drift and speed variation, trace density variations and the digitization process. This noise limits the range of ground motion for which useful data can be obtained. Generally speaking, the optical instruments will have difficulty pro-

viding useful data for earthquakes of M=4 or smaller even in the epicentral region and for earthquakes of magnitude M=6.5 if further than 200 km from the source.

Digital instruments have inherent advantages so far is noise is concerned. Noise associated with media drift, transport speed variation and trace density variation are essentially eliminated with the digital format. Furthermore, digitization error is greatly reduced by eliminating the intermediate step of optical recording.

In order to obtain quantitative data on the background noise of a typical digital strong-motion recorder, a Kinemetrics PDR-1/FBA-13 instrument was tested. The PDR-1 is a gain ranging recorder with 12 bit resolution and a 102 dB dynamic range. The FBA-13 is a three-component force balance accelerometer unit. The accelerometers nominally have a 50 Hz natural frequency and 70% damping and are capable of dc measurement. The transducers tested (Ser. Nos. 16345 and 16347) had a range of ±2g.

The FBA-13 transducer was mounted on an air suspension optical table in a quiet laboratory environment. Samples of background noise with a duration of 20 seconds were recorded using the PDR-1 "run" mode, and subsequently processed to obtain the time history of the noise and the pseudo-velocity response spectrum. Care was taken in balancing the transducer so that maximum system gain was obtained. No data was obtained at lower gains. The input low-pass filters of the recorder were set at their maximum value of 50 Hz and the sample rate was 200 sps. No correction was introduced into the processing except for a uniform baseline shift to eliminate the dc component of the accelerogram.

Figure 1 shows the time history of the background noise acceleration for four different test runs. It is seen that the noise is generally associated with fluctuations in the last bit of the digital data. Some low frequency drift is evident. Figure 2 shows the Fourier Amplitude Spectrum of one of the noise time histories of Figure 1. This spectrum was obtained using a Kaiser-Bessel filtered version of the data. The result shown is typical.

Figure 3 shows the superimposed zero-damped response spectra for the four different test runs. Also shown in Figure 3 is the band of average digitization noise plus one standard deviation for a typical hand digitized optical record as reported in the literature (Hudson, 1977; Hudson, 1979). In addition, the figure shows the 20% damped average digitization noise spectrum which is claimed for the automatic digitization system employed by the California Division of Mines and Geology.

It is seen from Figure 3 that there is a very striking difference in noise level between the analog and digital systems. The difference varies from more than one order of magnitude at short periods (high frequency) to about two orders of magnitude at long periods (low frequency). It is clear from the figure that the digital instrument is capable of accurately measuring the acceleration from much smaller events than the analog instrument. It is also clear that the digital instrument should give superior results for integrals of the acceleration; i.e., velocity and displacement. The digitization noise in the displacement at a period of ten seconds is of the order of two inches for the optical instrument but is closer to 0.02 inches for the digital instrument. It would therefore be anticipated that the digital instrument could be used to extract significantly more

-4-

information about displacement than the analog instrument. This possibility is examined in the next section.

COMPUTATION OF DISPLACEMENT FROM ACCELERATION

In principle, velocity and displacement time histories could be obtained directly from an acceleration time history by numerical integration. However, for optically recorded data, this usually results in errors which are unacceptably large. This is due to the fact that digitization and other errors associated with optical recording increase with period and therefore become amplified when the time history is integrated. In addition, an initial portion of the acceleration time history is lost in the analog instrument due to the finite time required to trigger this instrument. The digital instrument has a much lower inherent digitization noise. Furthermore, the pre-event memory incorporated into most instruments eliminates the ambiguity in the initial conditions of the record.

In order to examine the nature of the errors associated with integration of acceleration time histories obtained from digital instruments, a series of laboratory tests were conducted using the PDR-1/FBA-13 instrument. The transducer was moved horizontally in a straight line on a very flat, level surface through a known displacement. The recorder was triggered from the output of the accelerometer oriented in the direction of motion. The acceleration data was then integrated to obtain the time history of velocity and displacement. A typical result for a test with a relatively smooth displacement is shown in Figure 4.

For the test results shown in Figure 4, the actual permanent displacement of the transducer as 10±0.1 inches (25.4±0.3 cm). It is seen that the integrated acceleration time history gives an accurate measure of this permanent displacement. The only correction applied to the data was to adjust the zero offset of the accelerogram by the average value of the pre-event data (the first 1.0 seconds of the record were used for this average) and apply an instrument correction to remove transducer distortion. The input low-pass filter of the PDR-1 was set at 50 Hz and the sample rate was 200 sps. The PDR-1 does *not* have a high-pass filter, so the dc output from the accelerometers is retained. This is a necessary feature of the instrument if permanent displacement information is desired.

It would not be possible to generate a displacement time history like that shown in Figure 4 from an optical recording instrument due to absence of pre-event data and the presence of significant long-period noise. In an attempt to minimize the effect of these factors, optically recorded data is typically subjected to a number of corrections. These include baseline corrections and low- and high-pass filtering. In order to obtain a better understanding of the effect of these corrections, the acceleration time history of Figure 4 was processed using the standard correction algorithms employed in the report series entitled "Corrected Accelerograms" published by the California Institute of Technology (Trifunac and Lee, 1973). The results are shown in Figure 5. It is seen that the effect of the correction algorithm is to "level out" the displacement time history thus eliminating any permanent displacement and simultaneously reducing the magnitude of the dynamic displacement.

ANOMALIES IN THE DIGITAL INSTRUMENT

Unfortunately, the excellent results of double integration of the acceleration indicated in Figure 4 are not altogether typical. Rather extensive laboratory testing and field use of the FBA-13 transducer has revealed an anomaly which has a significant effect on data analysis. Figure 6 shows the result of direct numerical integration of a permanent displacement test in which the transducer was moved with a rather rough motion having associated high acceleration peaks. In this case, a very noticeable drift is observed in the displacement time history which completely overshadows the actual test permanent displacement which was again 25.4 cm.

Through further testing, it was determined that the baseline output of the FBA-13 could be observed to shift suddenly if a sufficiently large input acceleration pulse were applied. This shift may be associated with minute slippage in the flexure support of the transducer, or hysteretic behavior of the fine wires which attach to the moving transducer element. The phenomenon is not fully understood and is currently under further investigation by the manufacturer. However, the anomaly has a very strong effect on the acceleration data when it is double integrated.

An attempt has been made to develop a correction algorithm which can compensate for the observed anomaly without having an adverse effect on the ability of the instrument to predict permanent displacement. The proposed correction algorithm is quite simple and based on the perceived mechanism of the anomaly. The acceleration data is first corrected for the dc offset observed in the pre-event data. Typically, this is accomplished by performing a time average on only the first one-half of the pre-event

data in order to eliminate the possibility of including any actual earthquake data. Next, the final offset of the acceleration is determined. If there were no instrument anomaly, this offset should now be zero since the pre-event and final offsets should be equal. However, due to slippage or other effects, these offsets will not, in general, be the same. If the dynamic or oscillatory component of the acceleration at the end of the record is smaller than the final offset of the record, as in Figure 4, the acceleration record may be used directly to determine the final offset. However, it has been found that it is usually more accurate to estimate the final acceleration offset from the final slope of the velocity record since it has a relatively smaller oscillatory component. Normally, the last 15 seconds of the time history are adequate to determine the acceleration offset.

Finally, the cumulative effect of the transducer anomaly during the time of strong shaking is estimated from the offset in the final velocity. This is accomplished by assuming that the intermediate baseline shifts can, on the average, be replaced by a rectangular acceleration pulse which occurs during the strongest portion of the acceleration time history. The overall correction for the instrument anomaly is shown schematically in Figure 7.

The time t_1 and t_2 may be selected in a number of different ways and it has been observed that the final results are generally fairly insensitive to this selection. Experiments have shown that very little base line offset of the transducer occurs for accelerations less than 50 cm/sec^2. Therefore, one possible approach is to select t_1 and t_2 such that $a(t)$ is less than or equal to 50 cm/ sec^2 for all t on the interval (t_1, t_2). This approach (Option One) works well when there is known to be a real final net displace-

ment. Another approach would be to select t_1 as the time of the first significant acceleration pulse and then select t_2 so as to minimize the computed final displacement. This approach (Option Two) is useful when the existence of a final displacement is not known *a priori*. If there is a real final displacement, Option Two will usually yield a value of t_2 which is less than t_1, signifying that Option One is more reasonable.

The correction for the final offset is normally determined by a least-squares fit of the final portion of the velocity data of the form

$$v_c(t) = v_0 + a_f t \quad .$$

The intermediate range correction is determined from the relation

$$a_m = \frac{v_c(t_2)}{(t_2 - t_1)} \quad .$$

The result of applying the correction algorithm to the acceleration time history of Figure 6 is shown in Figure 8. Option One was used in the selection of t_1 and t_2. The corrected displacement results show good agreement with the actual permanent displacement of 25.4 cm. Very little low frequency (long period) information seems to have been lost from the data by the correction algorithm. Indeed, this was one of the goals in the development of the algorithm.

Additional examples of the results of prescribed displacement tests using the proposed correction algorithm are given in Figures 9-12. The FBA transducer was initially adjacent to a ruler and the recorder set in the "triggered" mode. The transducer was then moved slightly away from the ruler and translated parallel to the ruler. Finally, when the desired displacement was reached, the transducer was moved back against

the ruler. The test displacement in each case was 25.4±0.3 cm. No special fixtures were used to maintain a fixed orientation of the transducer while it was translated. Hence, angular rotation of the transducer may account for some of the differences between the actual and computed displacement. However, it is more likely that the single correction algorithm used is not adequate when large amounts of transducer baseline shift take place over a long duration.

Figure 9 shows the corrected version of the test shown in Figure 4. Figure 10 shows a similar test with a fairly smooth displacement. Figure 11 shows a test in which the motion was caused by a series of discrete impacts to the transducer. This test clearly illustrates both the nature of the hypothesized instrument anomaly and the limitations of the proposed simple correction algorithm. From the velocity time history, it is evident that there is a different transducer offset associated with each impulse. Averaging the effect of these individual shifts over the approximately 10 seconds of strong acceleration to obtain a single effective shift a_m as prescribed by Option One is not adequate for such a case. When the acceleration pulses are distinct, as in Figure 11, it is possible to apply an offset correction to each individual pulse in a manner analogous to that used in the simple correction. Figure 12 shows the results of using such an approach on the data of the test shown in Figure 11. The improvement in the computed time histories of the velocity and displacement is apparent.

Table 1 gives a summary of the values of the correction parameters and the final displacements obtained from double integration of the acceleration for the tests presented in Figures 8-12. It is seen that the numerical values of the corrections a_f and a_m

are generally quite small. The displacement results have been observed to be fairly insensitive to the selection of the threshold acceleration level which defines t_1 and t_2.

It is believed that the simplified correction algorithms will be adequate for most short-duration earthquake-like time histories of motion. In that case, the time duration over which the central correction is applied will generally be smaller than for the high level acceleration tests presented herein and the permanent ground displacement will also take place over a shorter time interval. This will be illustrated by examples which follow.

It should be emphasized that the suggested correction algorithm has been introduced only to eliminate an observed anomaly in the instrument. It is anticipated that the source of this anomalous behavior will soon be eliminated so that correction of the digital accelerogram will no longer be necessary.

COMPARISON OF ANALOG AND DIGITAL RECORDS

Following the Coalinga earthquake of May 2, 1983, a SMA-1 optical analog recording accelerograph and a PDR-1/FBA-13 digital accelerograph were installed side-by-side in a residential garage near the center of the city to measure aftershocks. On May 8, 1983, an aftershock of M_L=5.5 with an epicenter approximately 11 km to the north of the city was recorded simultaneously by both instruments. The results obtained represent a unique opportunity for a direct comparison between the optical analog and digital recording instruments.

The time histories of the ground acceleration, velocity and displacement for the digital instrument are shown in Figures 13-15. The time histories shown were corrected

using the algorithm described herein with t_1 and t_2 selected according to Option Two. The sampling rate was 100 sps.

The time histories obtained from the analog instrument are presented in Figures 16-18. These results were obtained from accelerograms which were digitized and corrected by the California Division of Mines and Geology. This data was band-pass filtered with a low frequency cut-off of 0.2-0.4 Hz and a high frequency cut-off of 23-25 Hz. The maximum acceleration, velocity and displacement obtained from the two different instruments are compared in Table II.

In general, there is rather close agreement between the results obtained from the analog and digital instruments. The greatest difference is, as expected, observed in the displacement. The results obtained from the digital instrument show the presence of a low frequency pulse with a duration of about 7 seconds while this pulse is filtered out of the results from the optical analog instrument. The potential of the digital instrument to provide long period displacement information is clearly indicated.

In order to obtain a more complete understanding of the difference between the analog and digital records, a correlation analysis was performed. The cross-correlation coefficient between each pair of records was computed and the time difference for maximum correlation determined. The analog record was shifted by this time difference and then subtracted from the digital record to obtain the time difference acceleration. The results are shown in Figures 19-21.

The difference acceleration shown in Figures 19-21 is somewhat larger than might have been anticipated from the relatively high correlation of the analog and digital

records. The most satisfactory explanation for this seems to be that there is a slowly varying phase shift with time between the two records. Whether this is associated with speed variations in the analog instrument, the digitization process or the instrument correction is uncertain.

In Table 3 the maximum correlation time difference for each pair of records is compared to the time difference between the largest acceleration peak of the records. In general, there is fairly close agreement between the two measures of time difference. This agreement holds as well for the difference between the largest velocity peak but not for the peak displacement.

The Fourier Amplitude Spectra of the digital, analog and difference acceleration time histories are shown in Figure 22-24. It is noteworthy that the Fourier Amplitude Spectrum associated with the difference acceleration is generally significantly larger than the difference between the Fourier Amplitude spectra of the digital and analog time histories. This is another indication of the presence of phase differences in the records that are not accounted for by a time shift corresponding to the maximum correlation time. Although not shown herein, a significant phase variation was also observed in the cross-spectrum of the digital and analog records even after the records were shifted.

The zero-damped response spectra for the three components of this aftershock are shown in Figures 25-27. The solid lines denote the spectra obtained from the digital instrument and the dashed lines denote the spectra obtained from the analog instrument. Two spectra are shown for each analog record. The higher response spectrum

values were obtained using corrected accelerograms which were high-pass filtered with a corner frequency of 0.07 Hz (14.3 sec period). The lower values were obtained using the accelerograms filtered with a corner frequency of 0.4 Hz (2.5 sec period) which are reproduced in Figures 16-18. It is understood that the corner frequency of 0.4 Hz was selected by the California Division of Mines and Geology to correspond approximately to the intersection of the 20% damped earthquake response spectrum and the nominal noise response spectrum (see Figure 3). There is very close agreement between the optical and digital response spectra for periods less than one second. However, there are some very significant differences in the range of periods greater than one second. The difference can be as large as an order of magnitude depending on the filtering used and the period considered. In this particular case, the optical instrument results are conservative compared to those of the digital instrument but this cannot be assured in general.

The spectral differences observed are believed to be caused by the presence of low frequency noise in the analog records which is not eliminated by the baseline and filtering corrections applied to this data. This conclusion is supported by the background noise level results presented in Figure 3. The absence of pre-event data along cannot account for the observed differences. The fact that the accelerograms filtered at 0.4 Hz have nearly the correct displacement asymptote appears to be coincidental.

From an engineering point of view, the comparison of the response spectra suggests that for an earthquake with this level of shaking, the optical instrument is capable of providing quite adequate estimates of the response of structures with periods less than

one second. However, the optical instrument data may lead to significant errors in estimates of the response of structures with longer periods even when the data is filtered according to accepted techniques. Additional data from side-by-side comparisons would be useful in extending these observations.

RESULTS FROM A RECENT CHINESE EARTHQUAKE

A number of PDR-1/FBA-13 instruments have been installed in China as part of a joint US/PRC cooperative project in strong ground motion measurement. This project is sponsored by the U.S. National Science Foundation and the Chinese State Seismological Bureau through the Instate of Engineering Mechanics in Harbin. A number of instruments have been installed in arrays in the aftershock region of the 1976 Tangshan earthquake. On October 19, 1982 a $M_s=5.3$[*] event occurred near the city of Lulong northeast of Tangshan. The location of the epicenter of this aftershock and the locations of instruments recording the event are shown in Figure 28. The epicentral location shown was determined by analysis of the strong-motion array data. The focal depth was estimated at approximately 10 km and the closest instrument (TS-12) was 4.2 km from the postulated epicenter. A comprehensive study of the aftershocks of this event has been made by Wu (1984).

The accelerograms obtained from station TS-12 are shown in Figures 29-31. The results shown are quite unique in that one channel of the horizontal data was not recorded at all during the earthquake due to an instrument malfunction. This data was

---

[*] This event was originally assigned a magnitude of ML=6.2 by the Chinese Institute of Geophysics but has recently been downgraded.

reconstructed later using the parity information recorded by the PDR-1. Time histories of the velocity and displacement are also shown in Figures 29-31. All of the records were processed using the correction algorithm described herein. However, due to the presence of some obviously incorrect data (and associated parity errors) early in the pre-event data, this data was averaged from 1.0 to 2.5 seconds. Application of Option Two for the selection of t_1 and t_2 yielded $t_2 < t_1$. Therefore, a form of Option One was used. The final result was insensitive to the precise values of t_1 and t_2 selected.

The results shown in Figures 29-31 predict a net horizontal absolute permanent displacement in the direction S30E of 4.0 cm and a net downward vertical permanent displacement of 1.0 cm. The rise time associated with the permanent displacement is of the order of 1.5 sec. All of these results appear to be consistent with the known fault behavior in the region and are not inconsistent with the predictions of theoretical source models for an event of this magnitude. To the authors' knowledge, this is the first time that such absolute ground displacement has been recovered from recorded data. Results of this type present a unique opportunity for the calibration of seismic source models.

CONCLUSIONS

Based on the observations reported herein, it is believed that the digital accelerograph will eventually become the standard instrument for strong-motion measurement. Even allowing for anomalies which exist in some current instruments, it appears that the digital instrument is capable of providing accurate data over a much wider range of amplitude and frequency than was previously thought possible. Expanded use

of digital instruments could have a beneficial impact on source modeling and wave propagation studies as well as structural response studies.

REFERENCES

Hudson, D.E. (1979). *Reading and Interpreting Strong Motion Accelerograms*, Earthquake Engineering Research Institute, Berkeley.

Hudson, D.E. (1977). "Reliability of Records," Panel 1, Earthquakes, *Proc. Sixth World Conf. on Earthquake Engr.*, New Delhi, India.

Trifunac, M.D. and V. Lee (1973). *Routine Computer Processing of Strong-Motion Accelerograms*, Earthquake Engineering Research Laboratory Report No. 73-03, Calif. Inst. of Tech., Pasadena.

Wang, P., L. Song and F.T. Wu 91984). Near Field Seismic Observation with a Mobile Little Aperture Network, *Proc. of International Workshop on Earthquake Engineering*, Shanghai, China, March 27-31, 1984.

ACKNOWLEDGMENT

TABLE 1. RESULTS OF DISPLACEMENT TEST

Test (Fig. No.)	a_f (cm/sec²)	a_m (cm/sec²)	t_1 (sec)	t_2 (sec)	Comp. Final Displ. (cm)
8	-6.52	-7.52	2.03	7.48	23.7
9	-0.081	-0.08	2.13	5.78	25.8
10	-0.09	-0.18	1.98	3.92	25.8
11	—	—	—	—	15.5
12	-1.10	—	—	—	25.9

TABLE 2 COMPARISON OF OPTICAL AND DIGITAL VALUES OF PEAK ACCELERATION, VELOCITY AND DISPLACEMENT – COALINGA AFTERSHOCK, MAY 8, 1984

	COMPONENT	DIGITAL REC.	OPTICAL REC.
Max. Accel. cm/sec²	N35E	99.5	95.7
	Up	73.3	-72.7
	S55E	117.3	114.6
Max. Vel. (cm/sec)	N35E	7.37	6.75
	Up	2.17	2.20
	S55E	4.46	4.11
Max. Displ. (cm)	N35E	0.97	-0.39
	Up	0.4	-0.17
	S55E	0.63	0.36

TABLE 3. COMPARISON OF TIME DIFFERENCE BETWEEN ANALOG AND DIGITAL

| | Time Difference (sec, ±0.01 sec) | |
Component	From Max. Correlation	From Max. Accel. Peak
35 Deg.	4.06	4.05
Up	4.06	4.01
125 Deg.	4.05	4.04
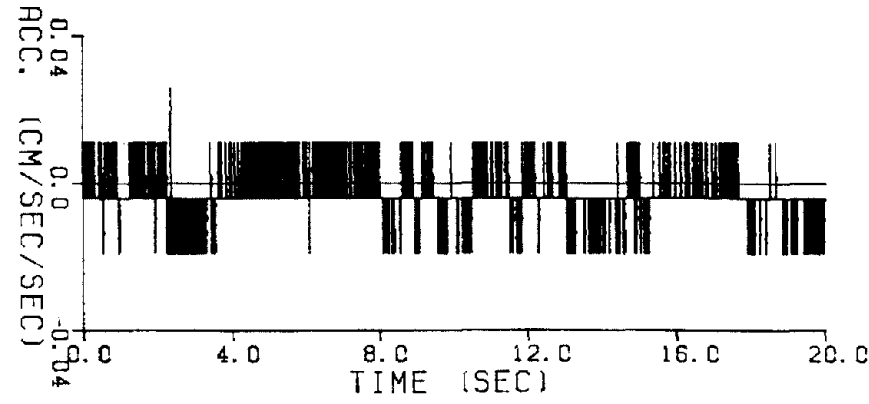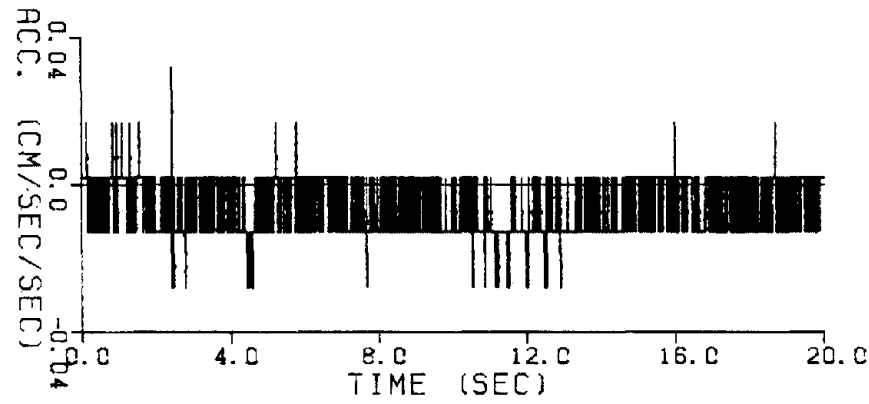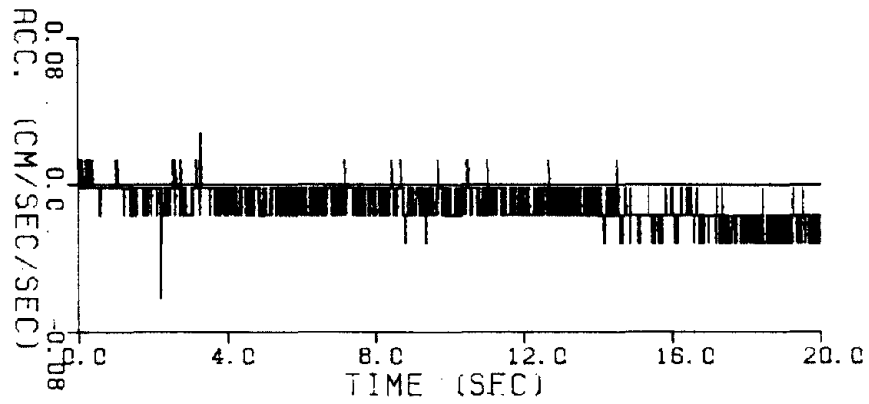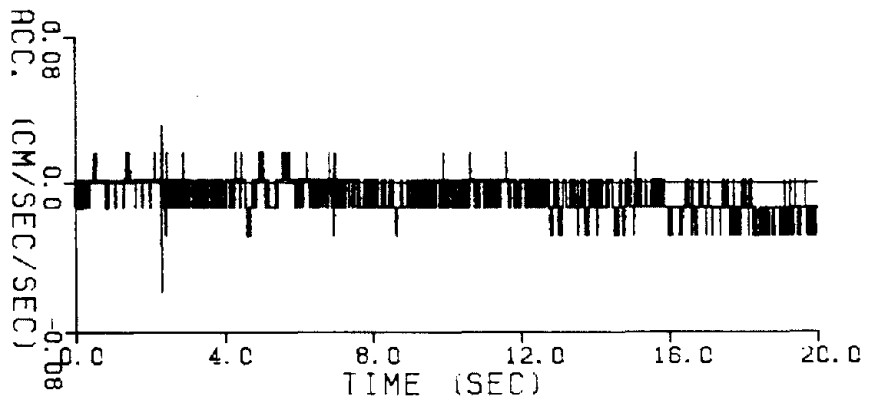
Figure 1   Acceleration Noise Time Histories
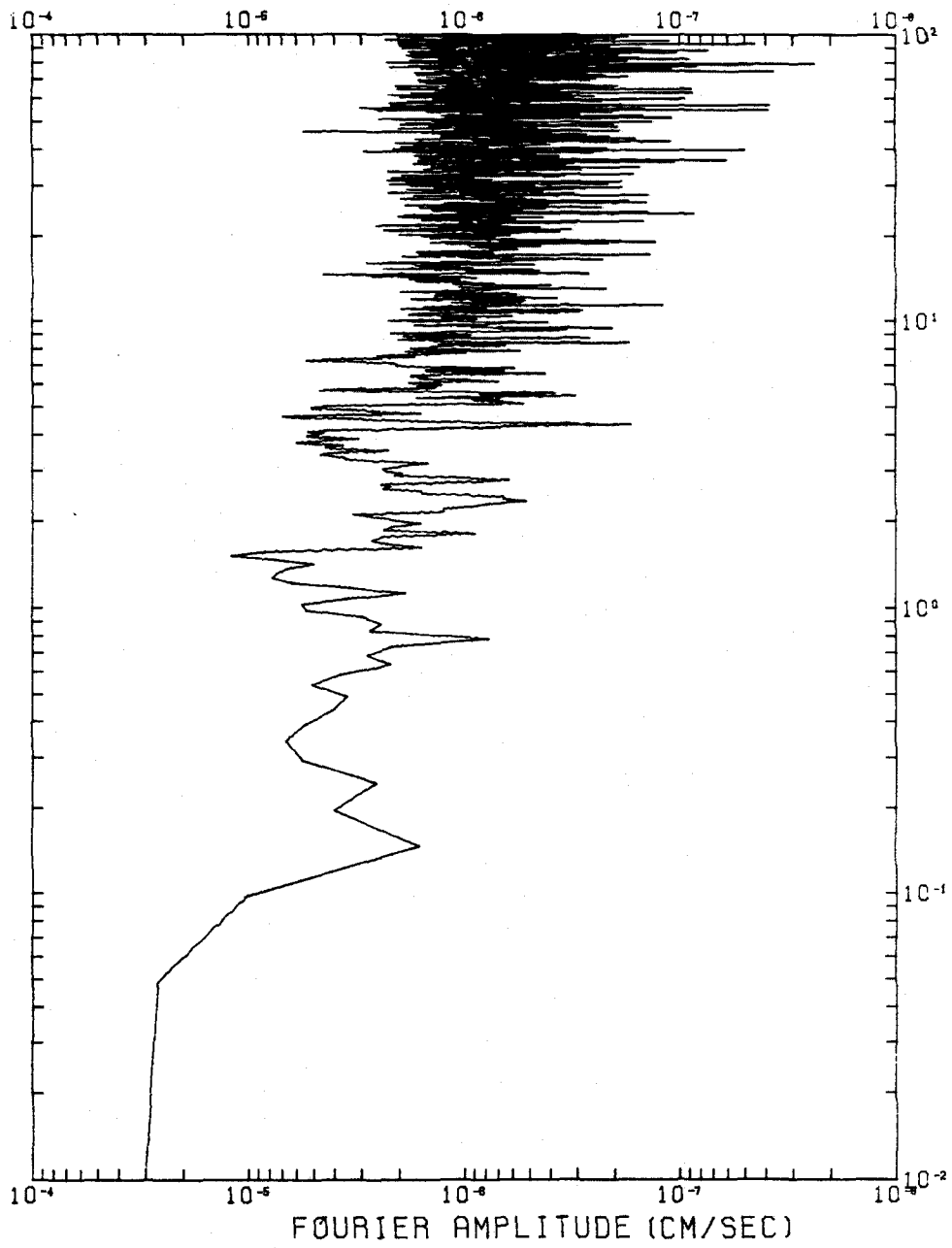
Figure 2 Fourier amplitude spectrum of noise record. Kaiser-Bessel filtered.
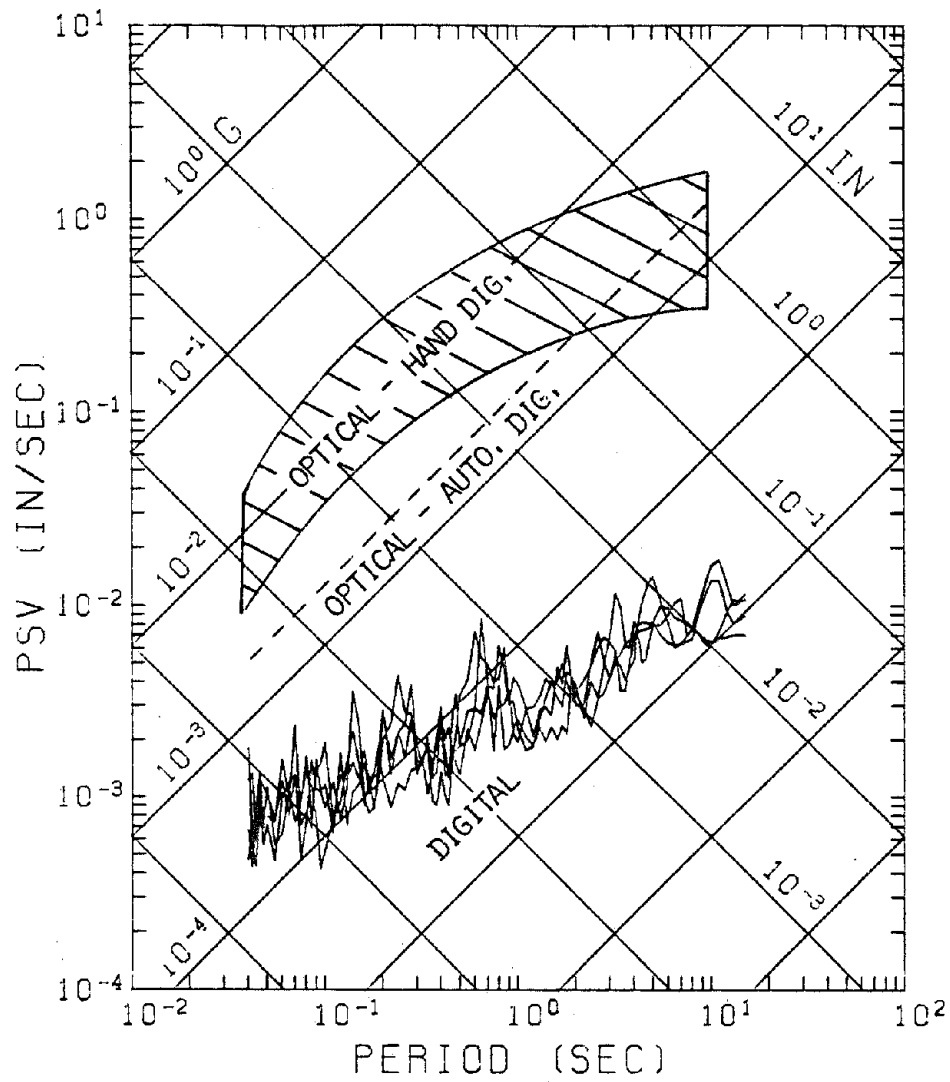
Figure 3   Response spectrum of background noise.
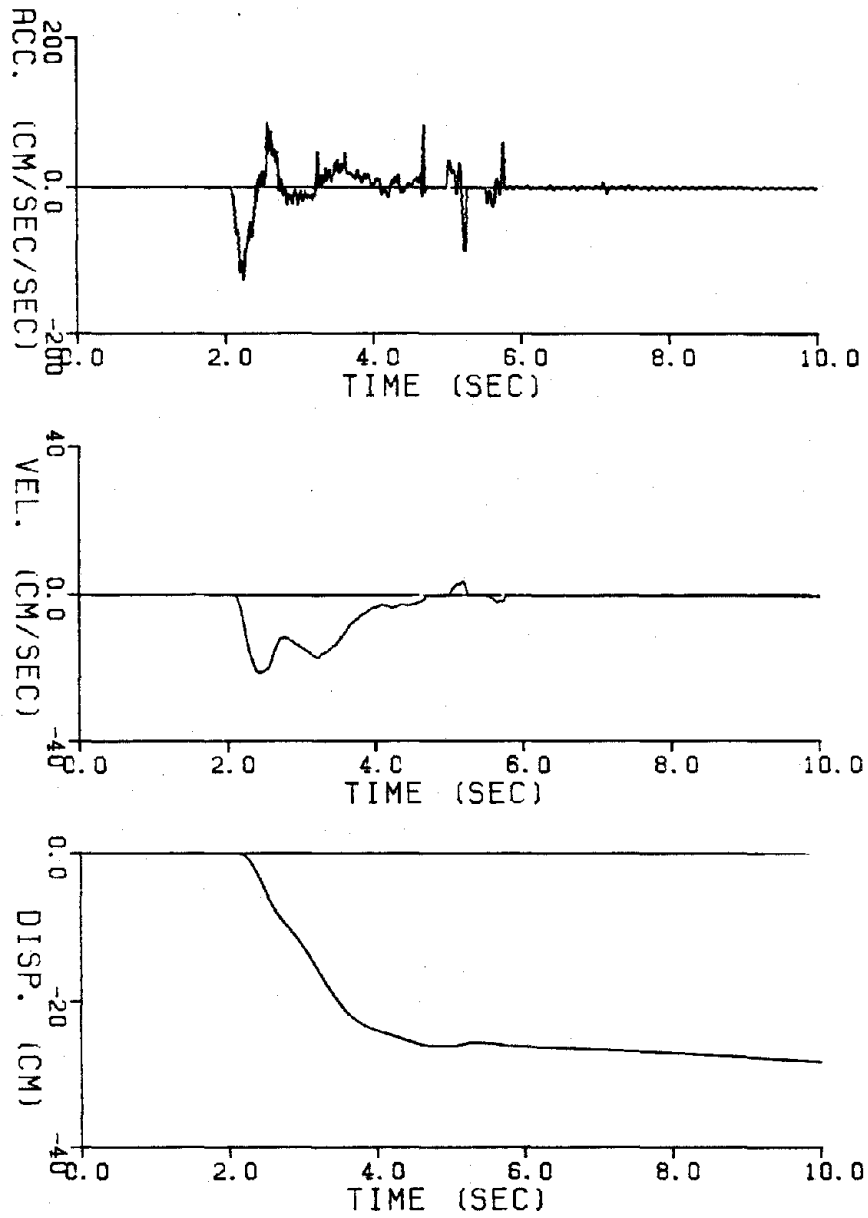
Figure 4   Displacement test – no data correction
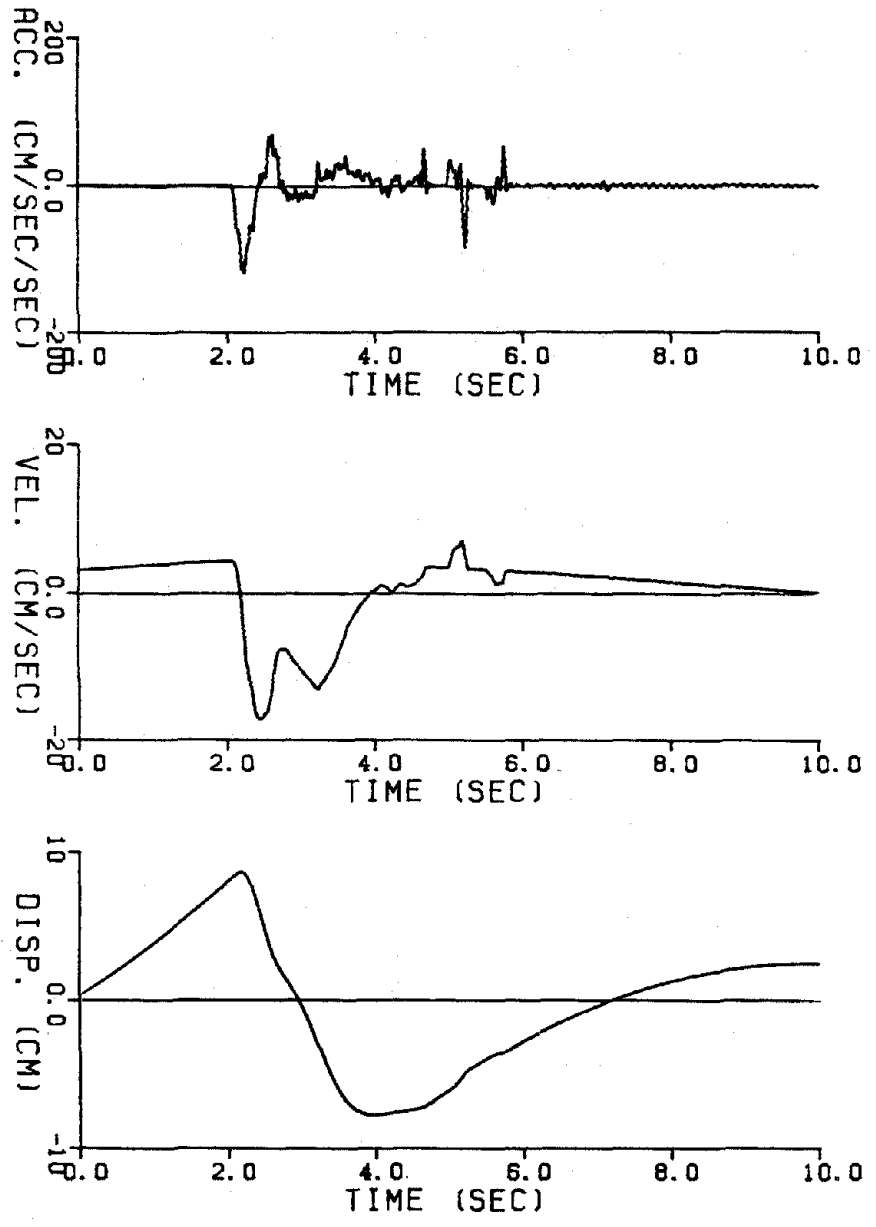
Figure 5   Displacement test of figure 4 with standard
           CIT Volume II correction.
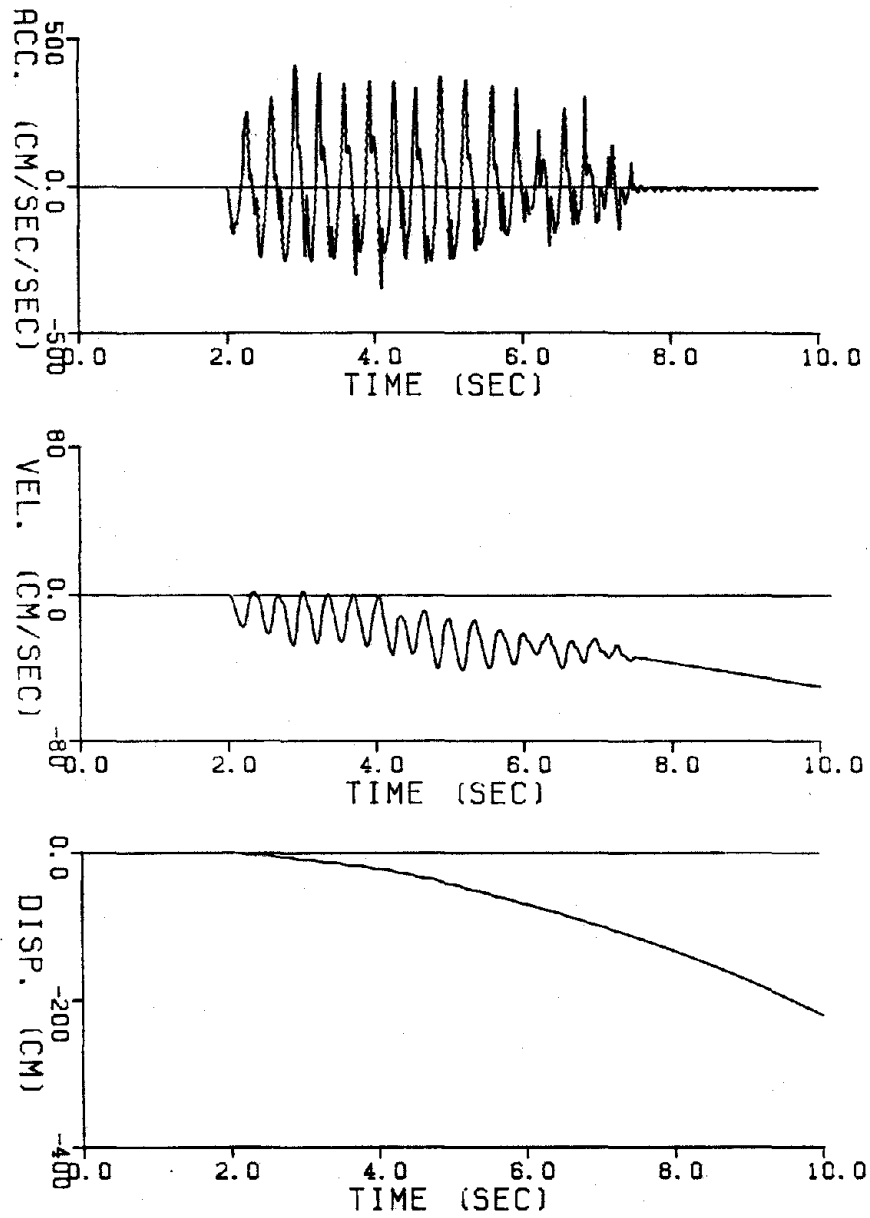
Figure 6   Displacement test showing effects of instru-
           ment anomaly.
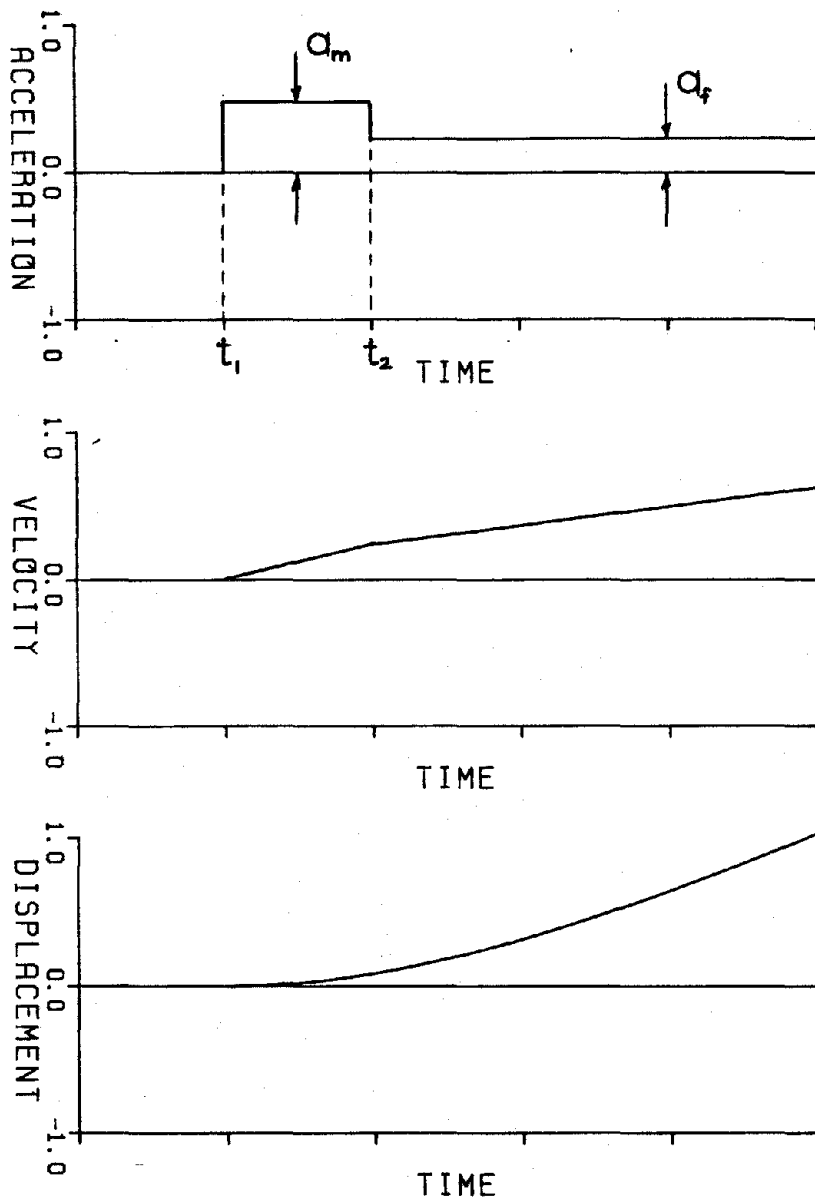
Figure 7   Simple correction algorithm for instrument
anomaly.
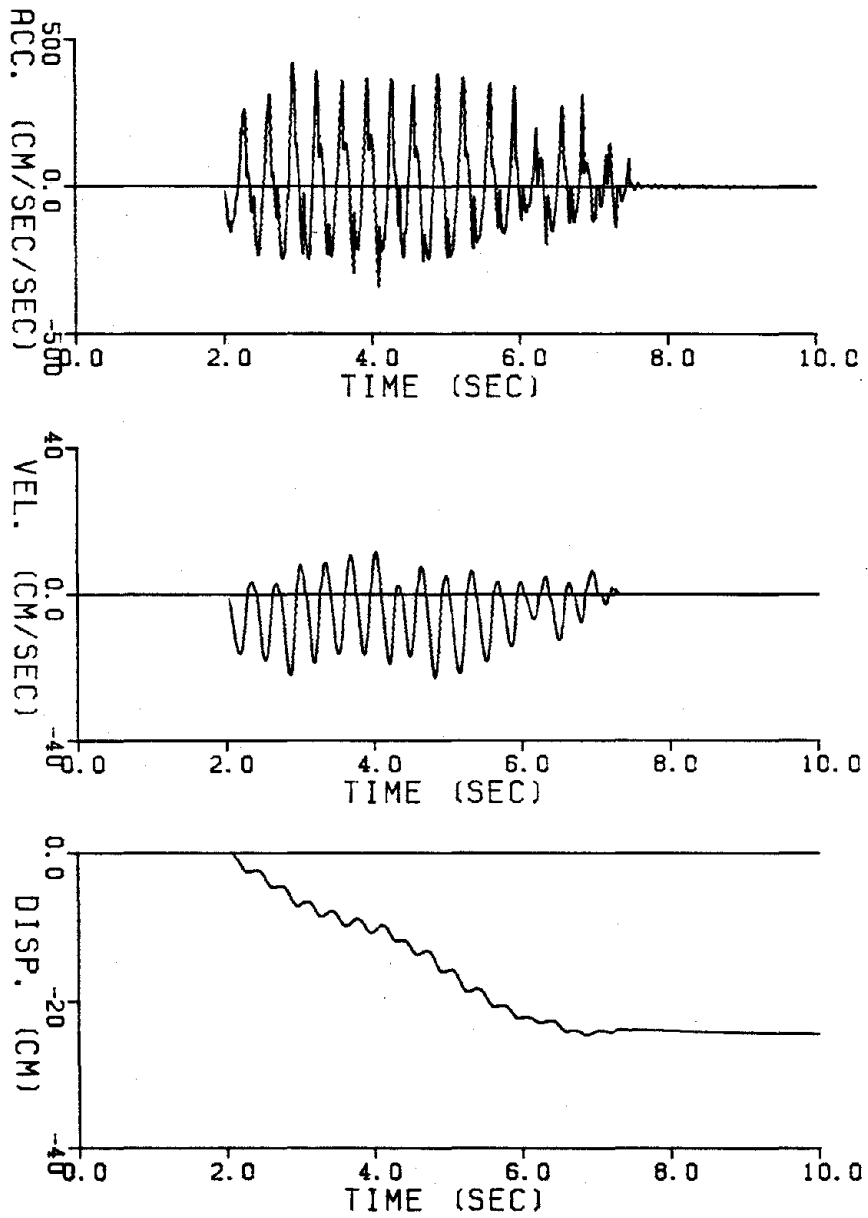
Figure 8   Displacement test of Figure 6 with proposed
           correction algorithm
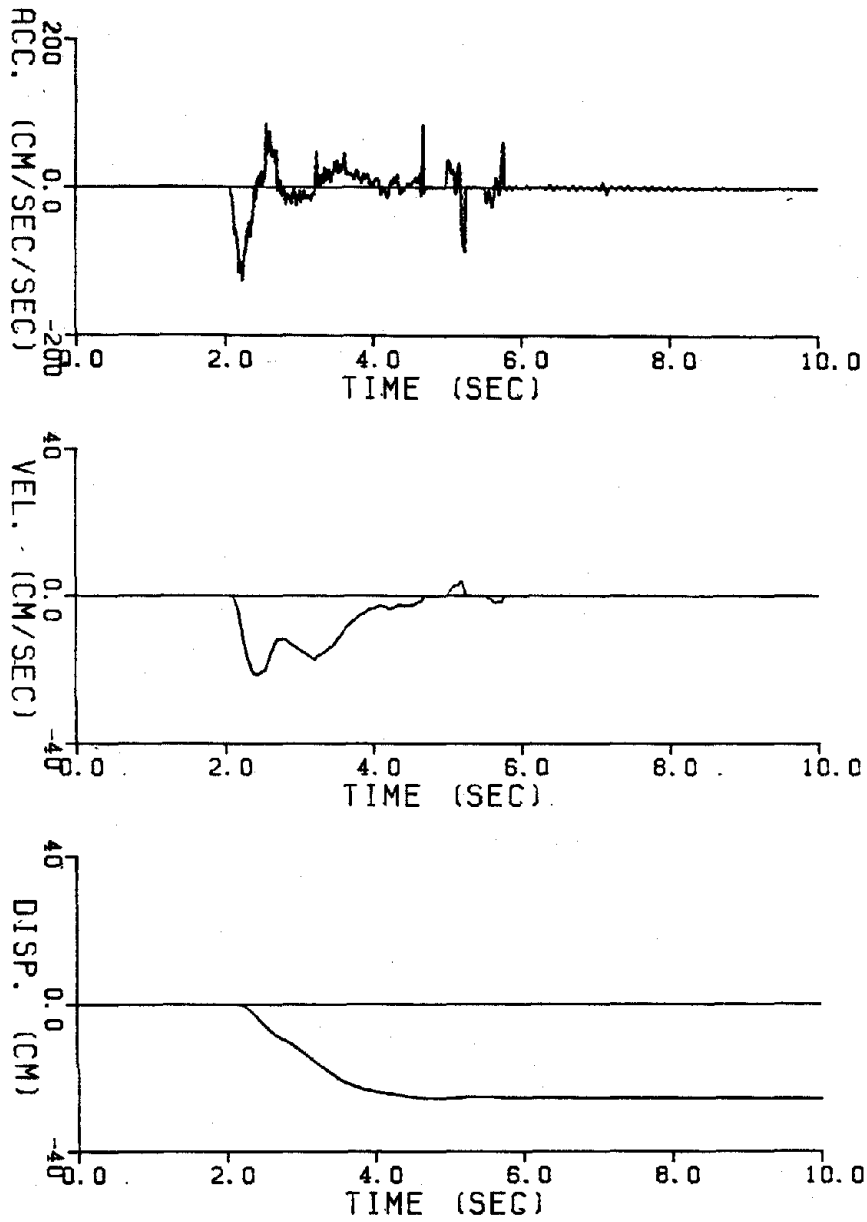
Figure 9   Displacement test of Figure 4 with proposed
           correction algorithm.
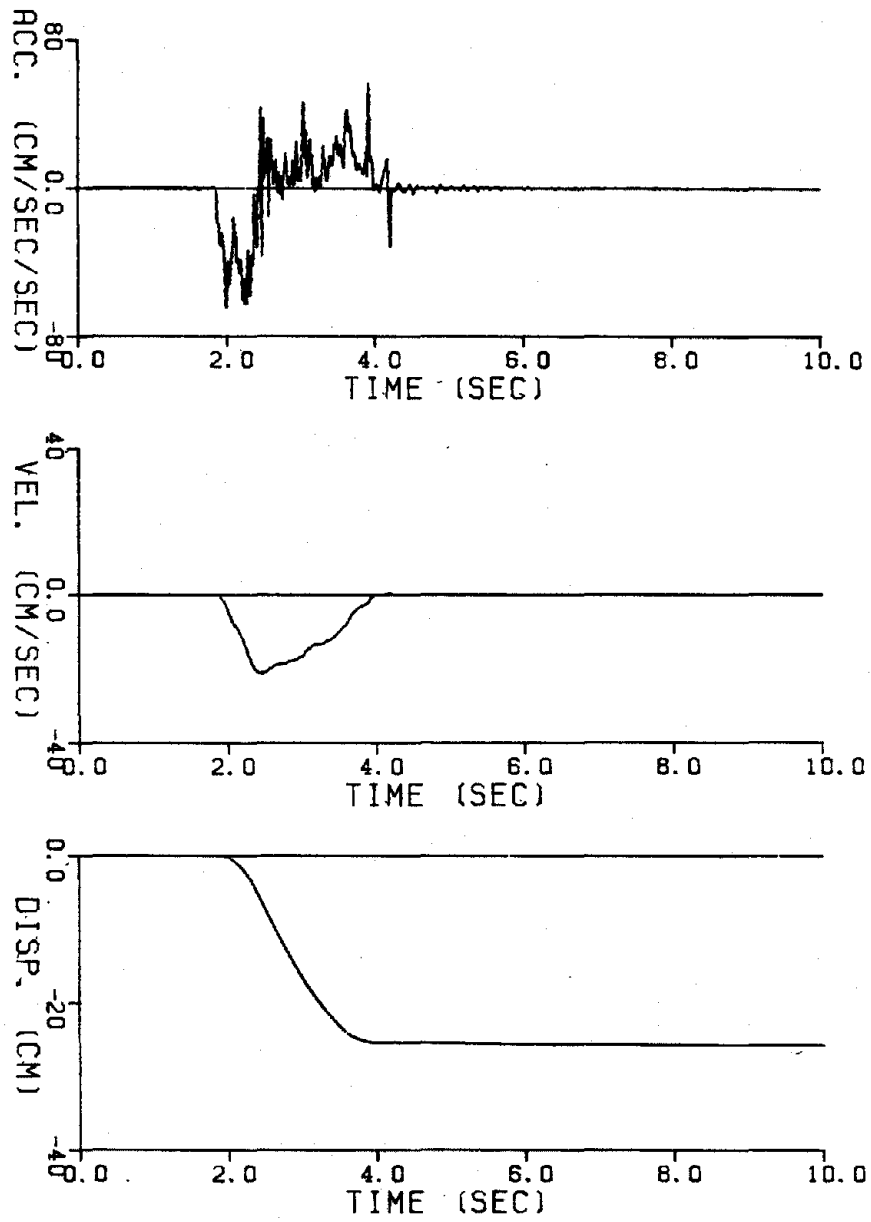
Figure 10   Displacement test with proposed correction algorithm.
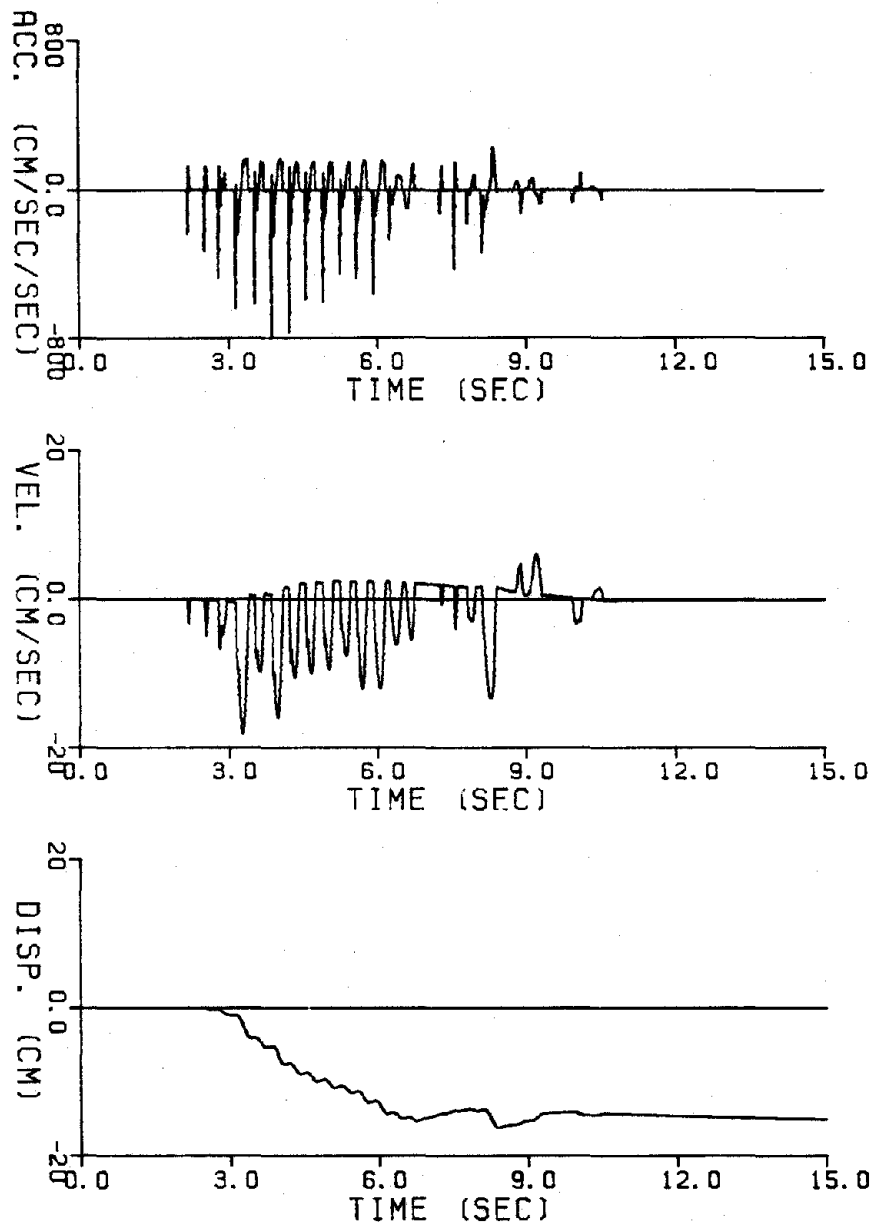
Figure 11 Displacement test with proposed simple correction algorithm.
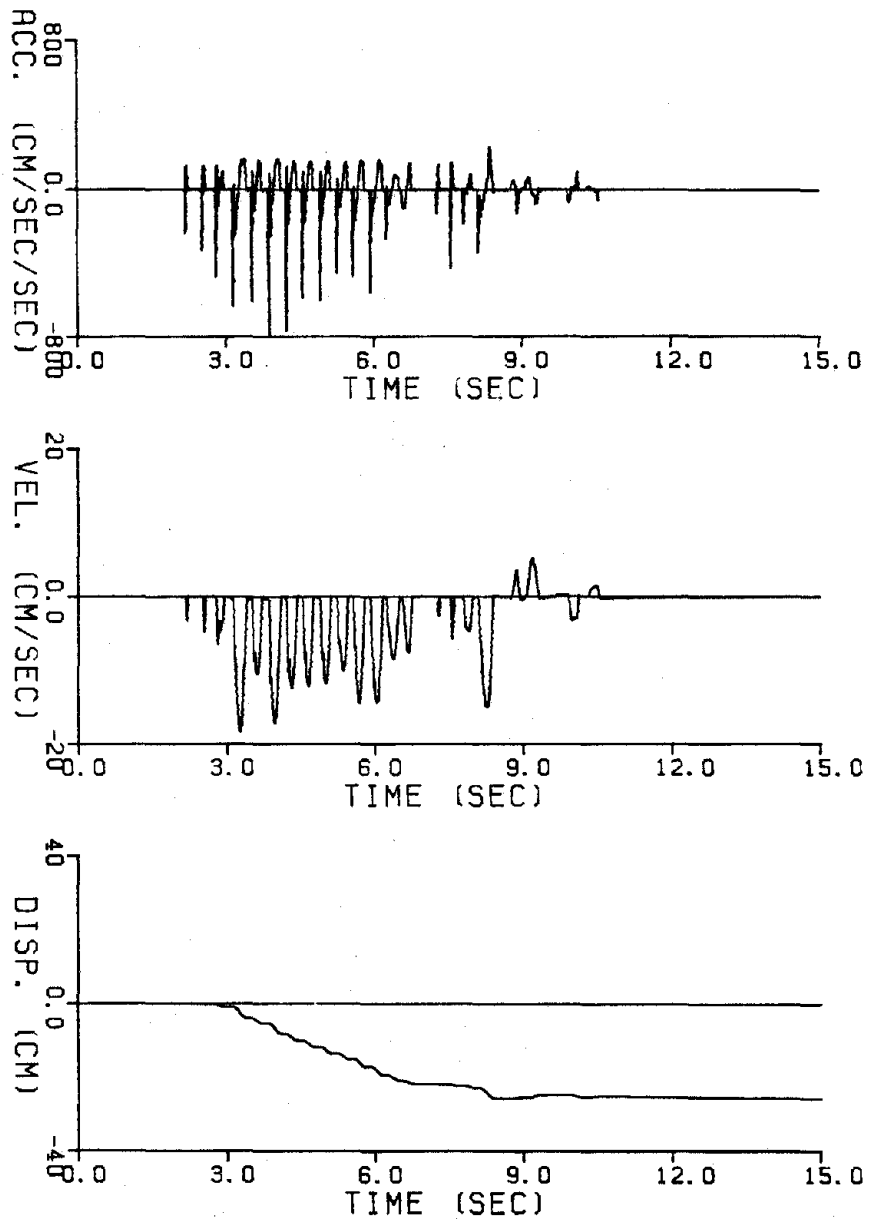
Figure 12 Displacement test of Figure 11 with more ex-
tensive correction.

COALINGA AFTERSHOCK MAY 8, 1983
DIGITAL RECORD 35 DEG
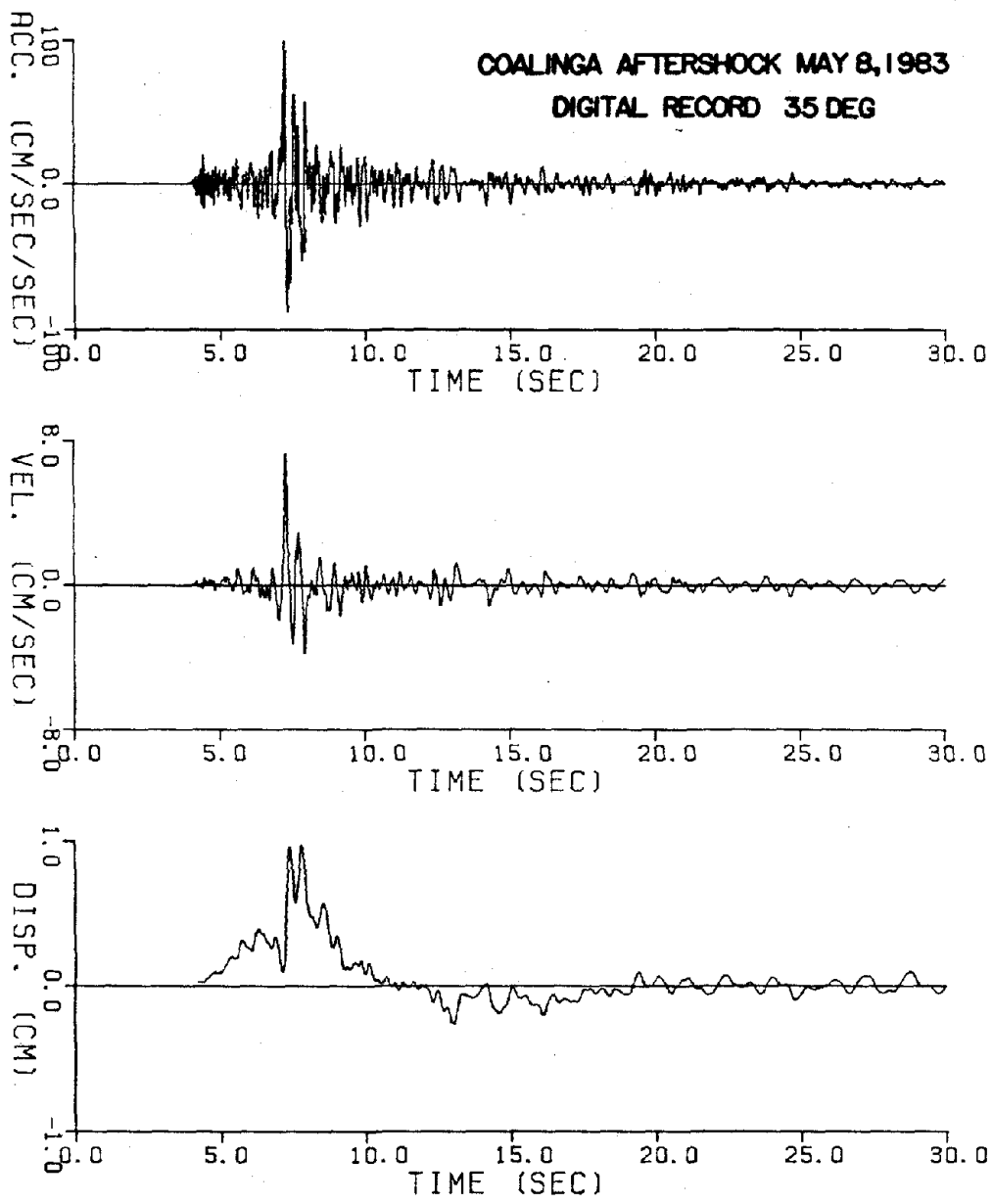
Figure 13   Digital accelerogram with integrated velocity and
            displacement. Coalinga aftershock of May 8, 1983;
            35 degrees.

ACC. (CM/SEC/SEC)

COALINGA AFTERSHOCK MAY 8,1983
DIGITAL RECORD UP

TIME (SEC)

VEL. (CM/SEC)

TIME (SEC)

DISP. (CM)

TIME (SEC)
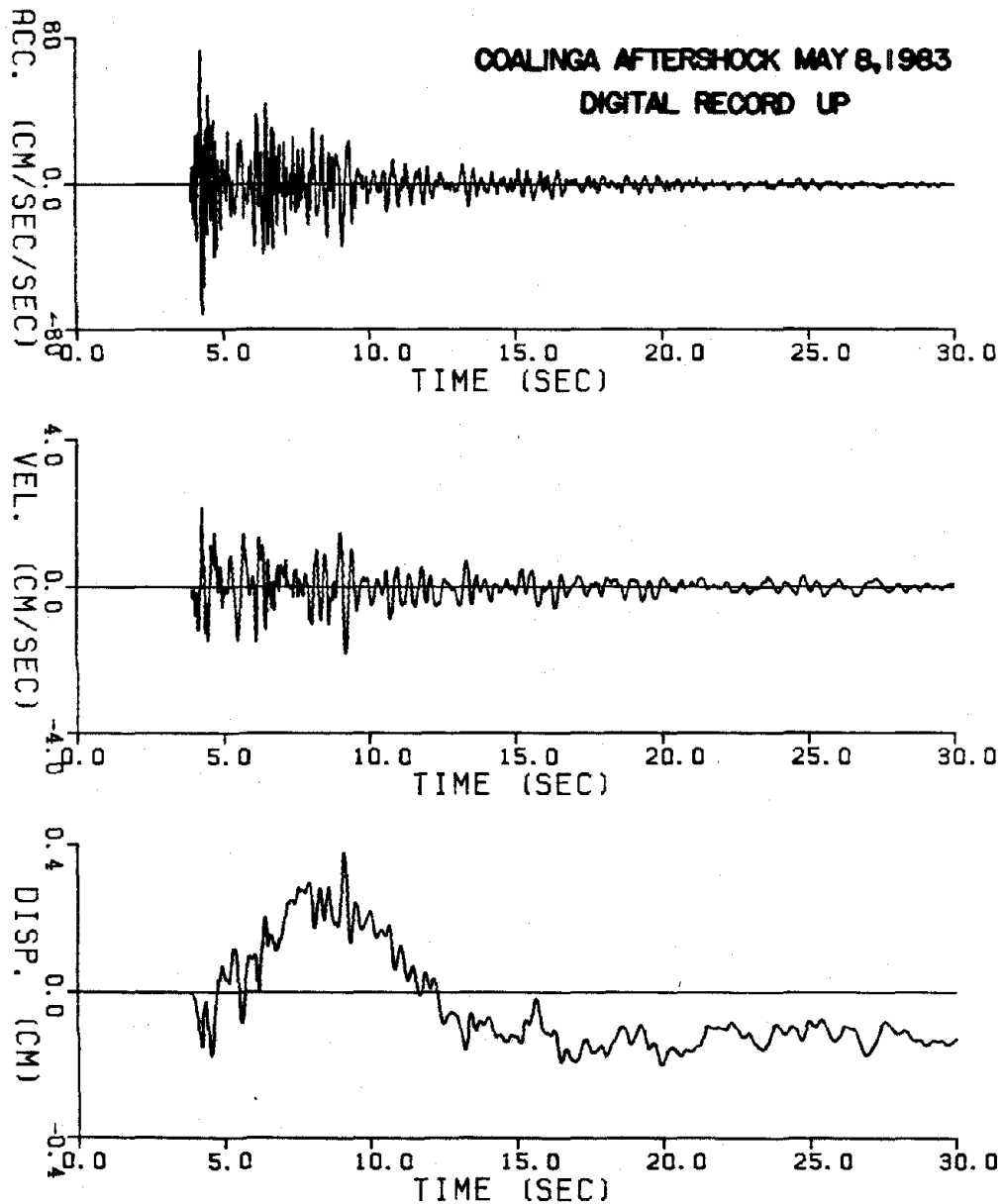
Figure 14   Digital accelerogram with integrated velocity and
displacement. Coalinga aftershock of May 8, 1983;
up.
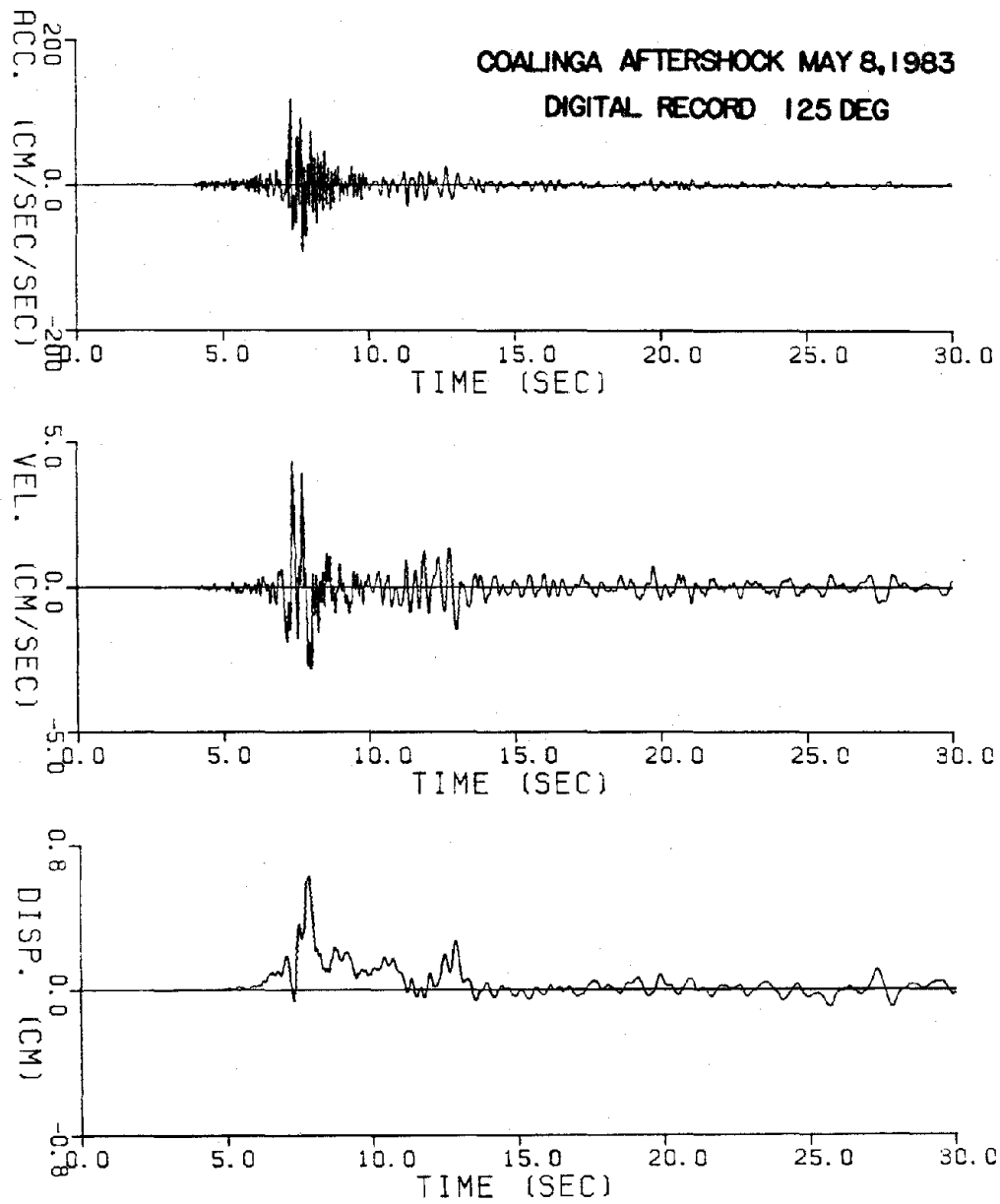
Figure 15   Digital accelerogram with integrated velocity and
displacement.   Coalinga aftershock of May 8, 1983;
125 degrees.
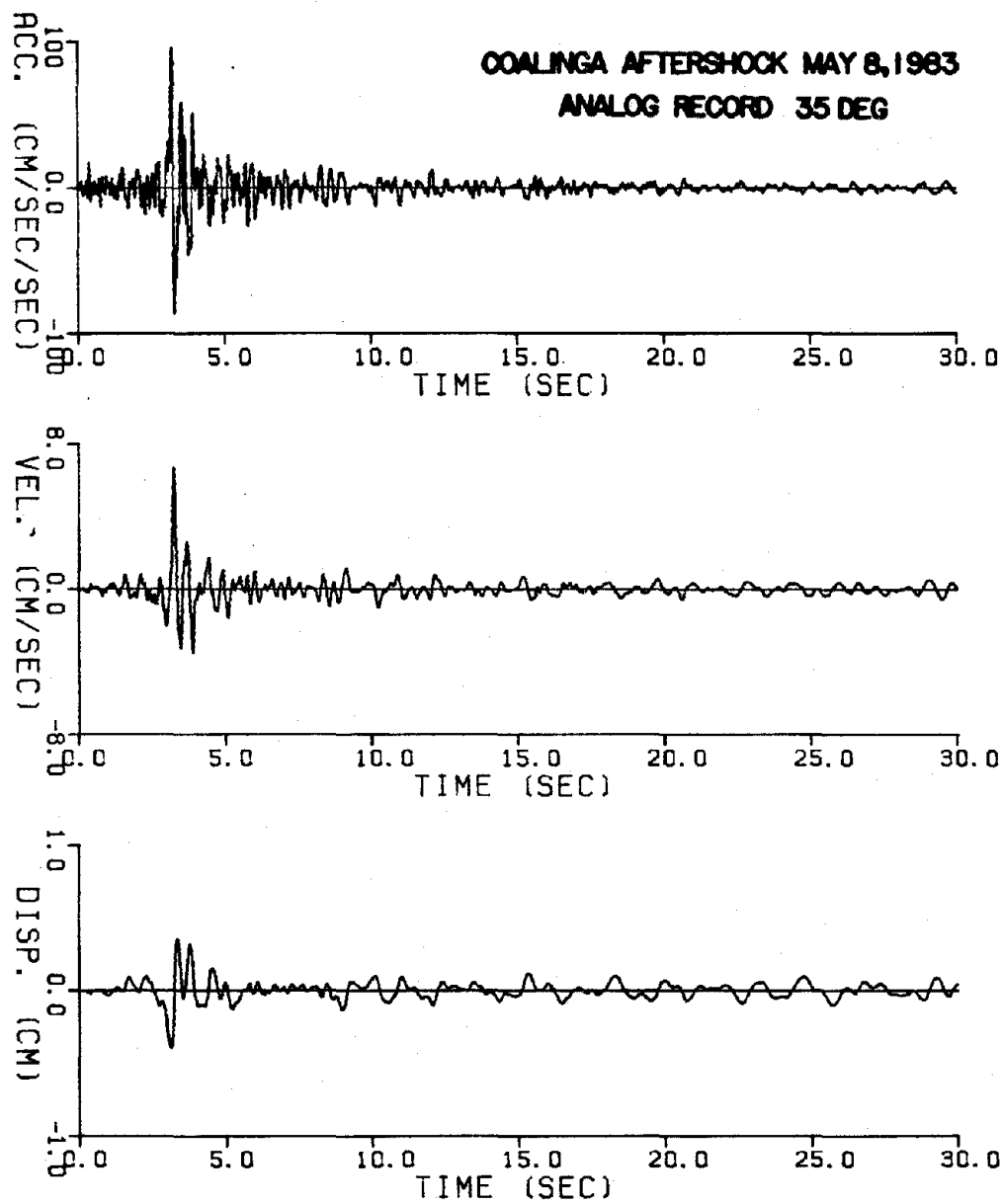
Figure 16   Analog accelerogram with integrated velocity and dis-
placement.   Coalinga aftershock of May 8, 1983;
35 degrees.
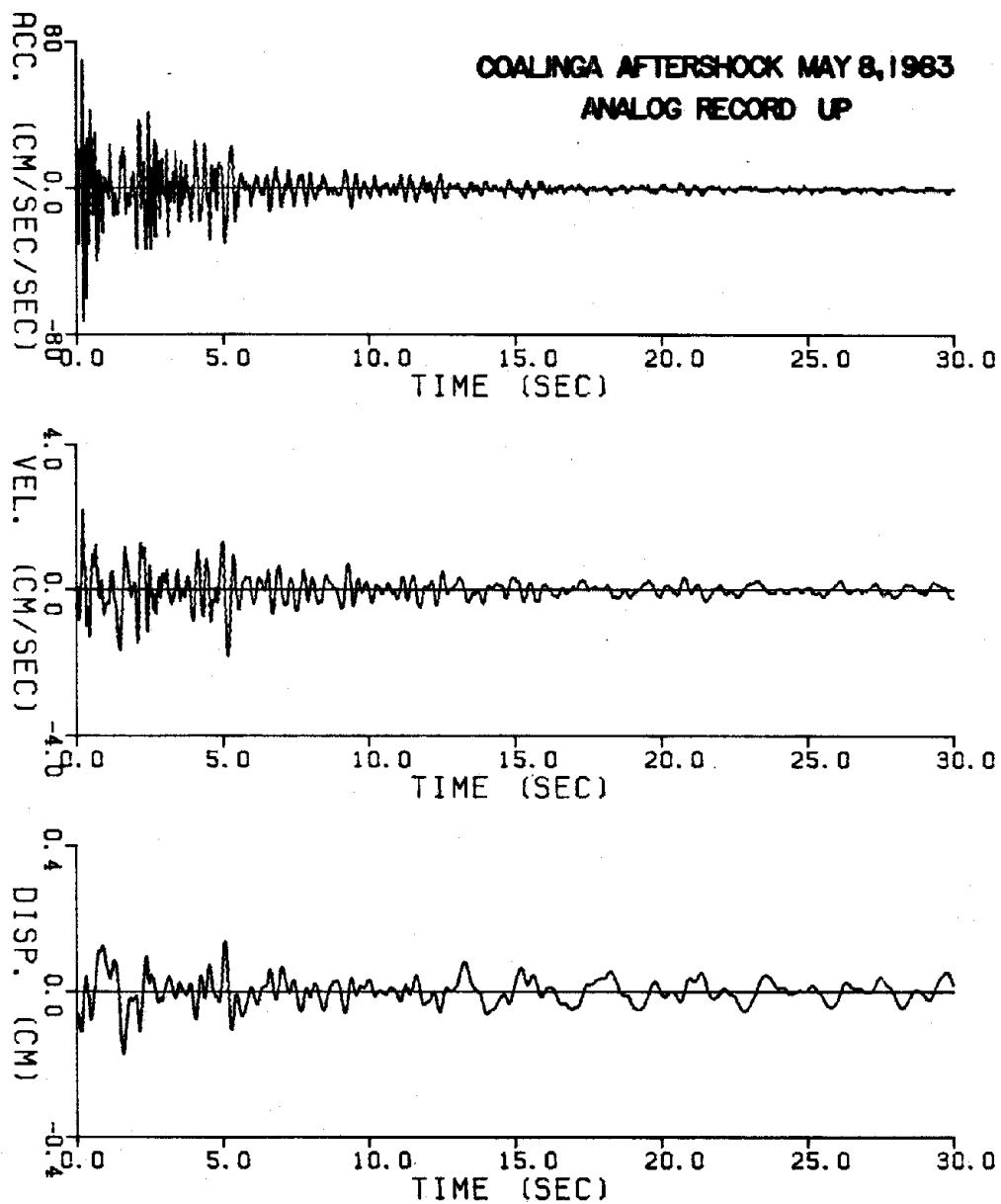
Figure 17 Analog accelerogram with integrated velocity and displacement. Coalinga aftershock of May 8, 1983; up.
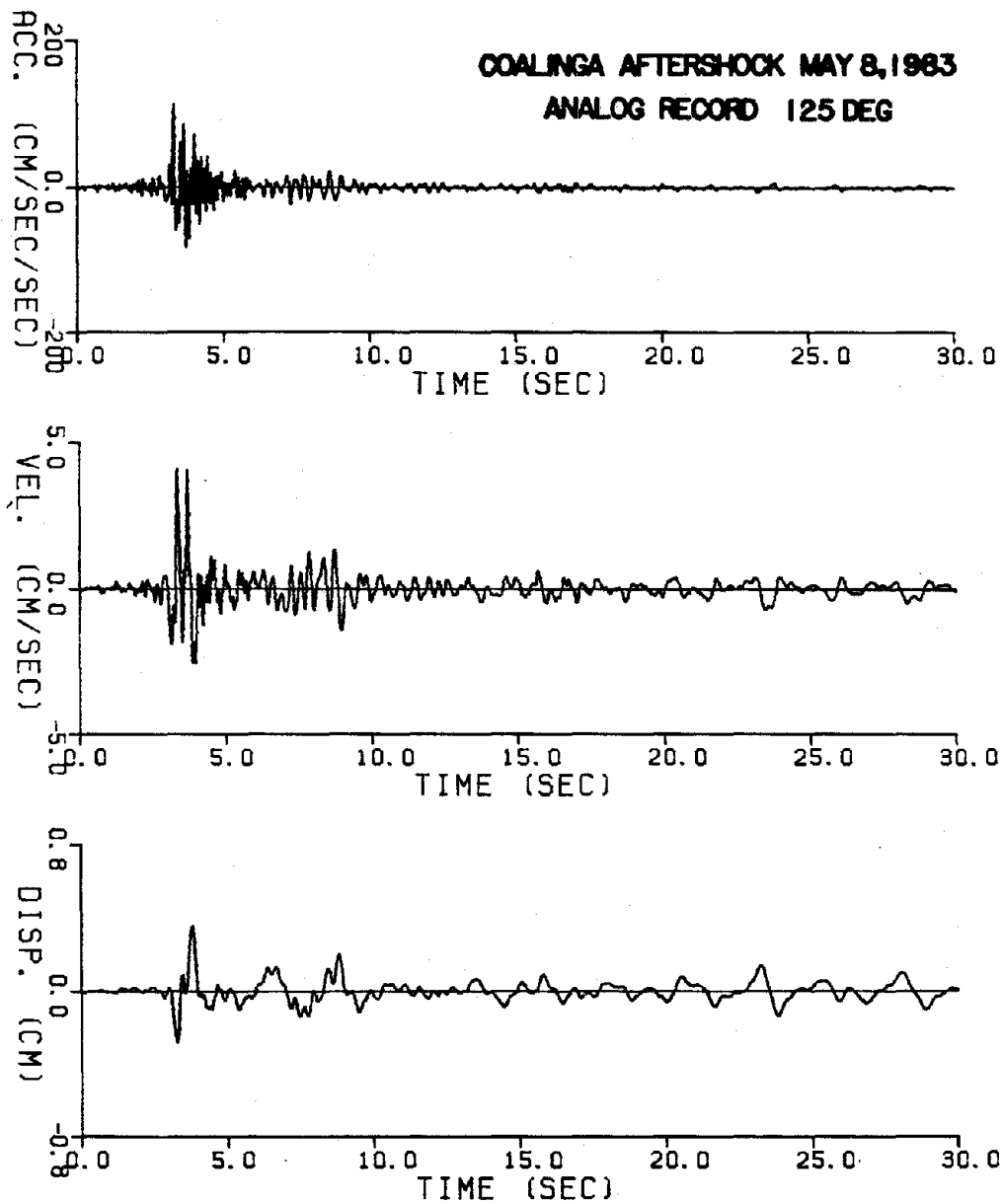
Figure 18   Analog accelerogram with integrated velocity and displacement.   Coalinga aftershock of May 8, 1983;
125 degrees.
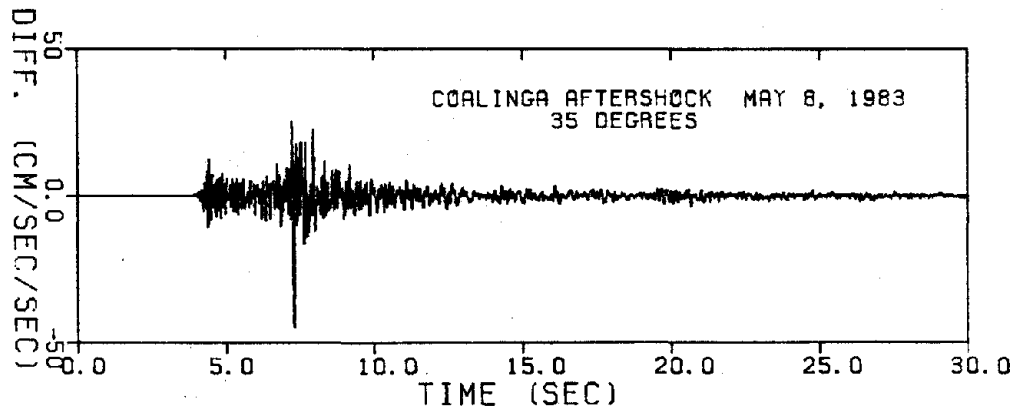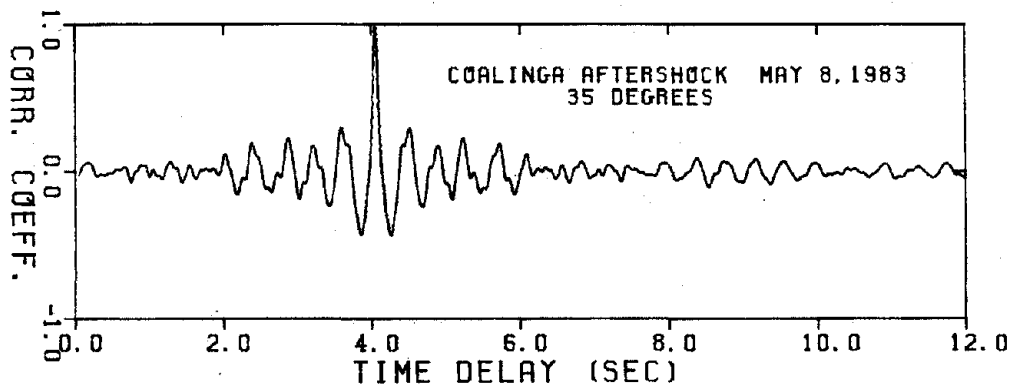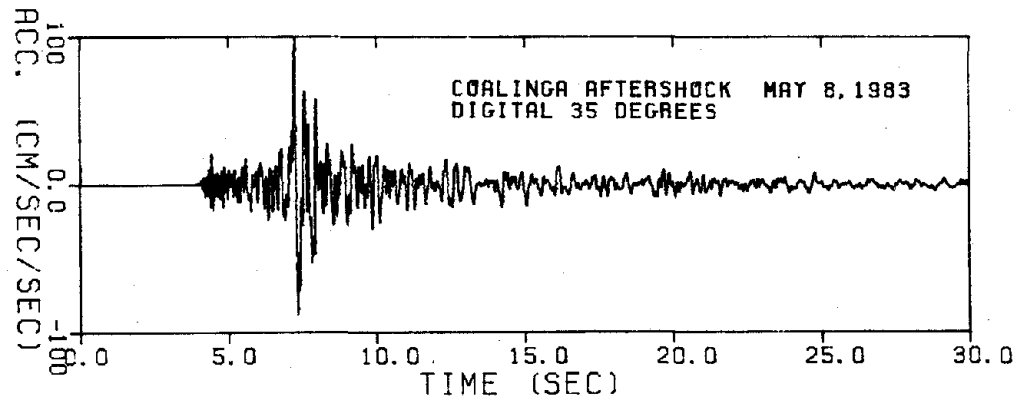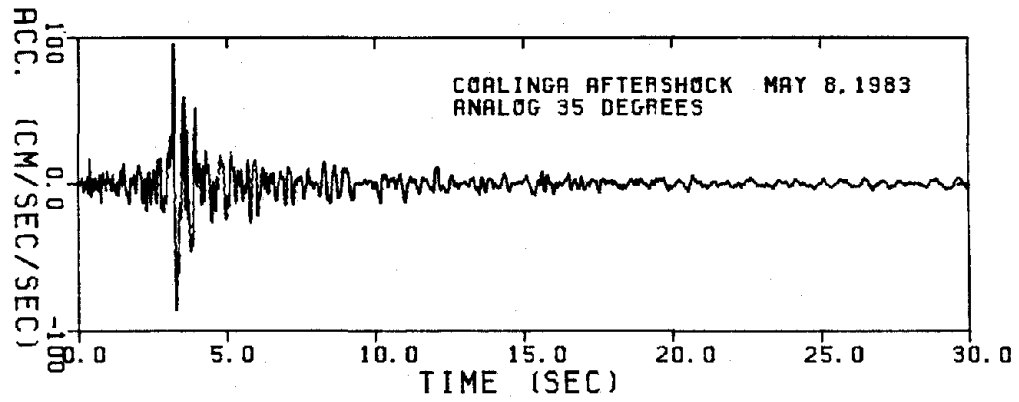
Figure 19   Correlation coefficient and difference between digital and analog
            accelerograms.   Coalinga aftershock, May 8, 1983; 35 degrees.
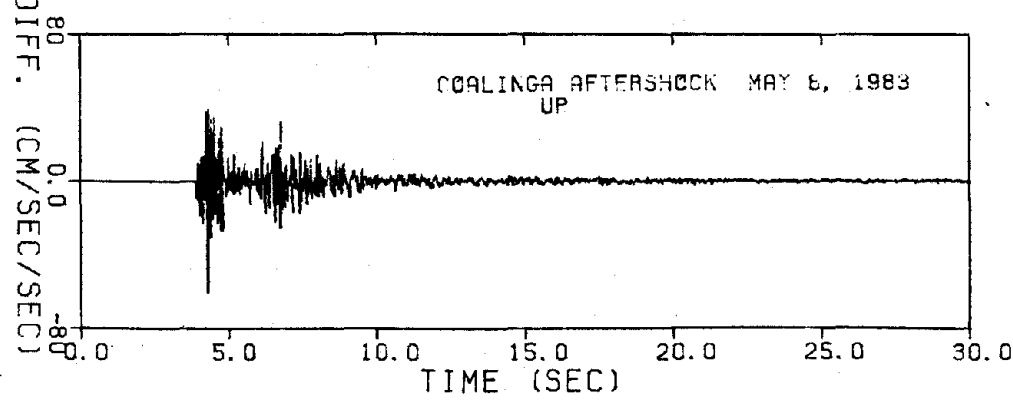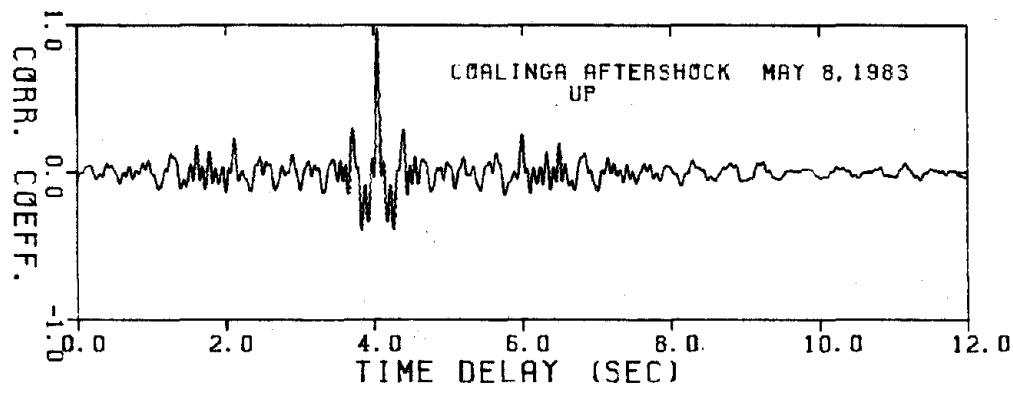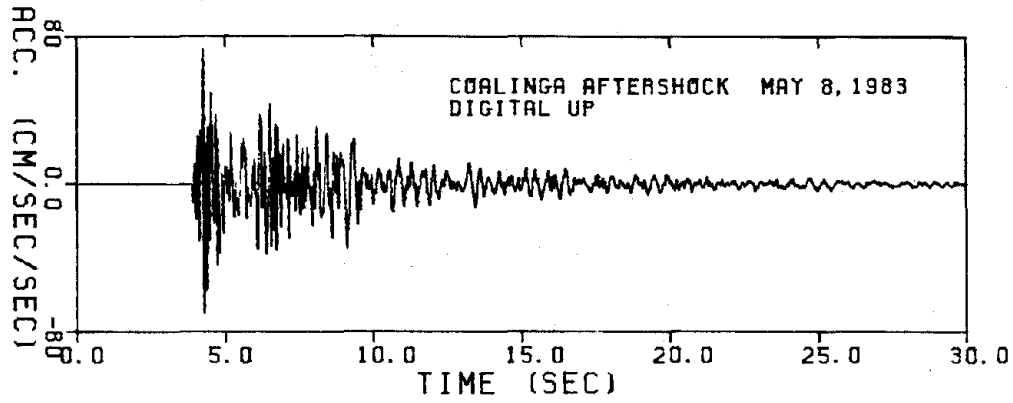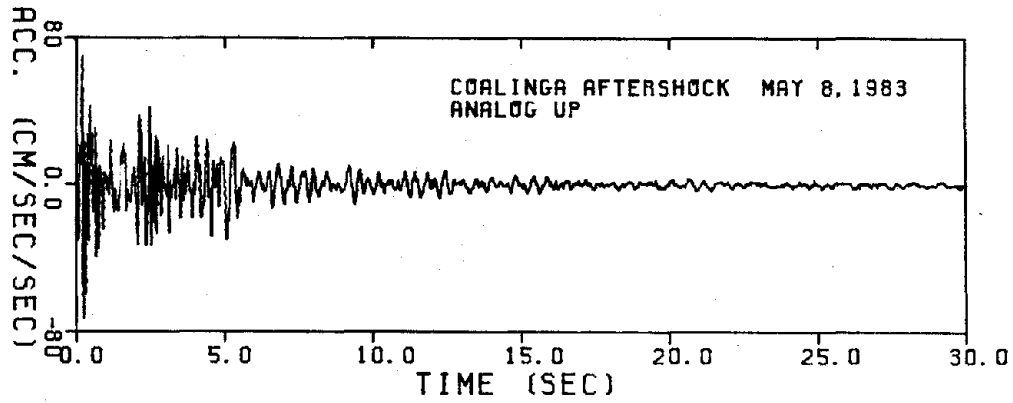
Figure 20 Correlation coefficient and difference between digital and analog
accelerograms. Coalinga aftershock, May 8, 1983; up.
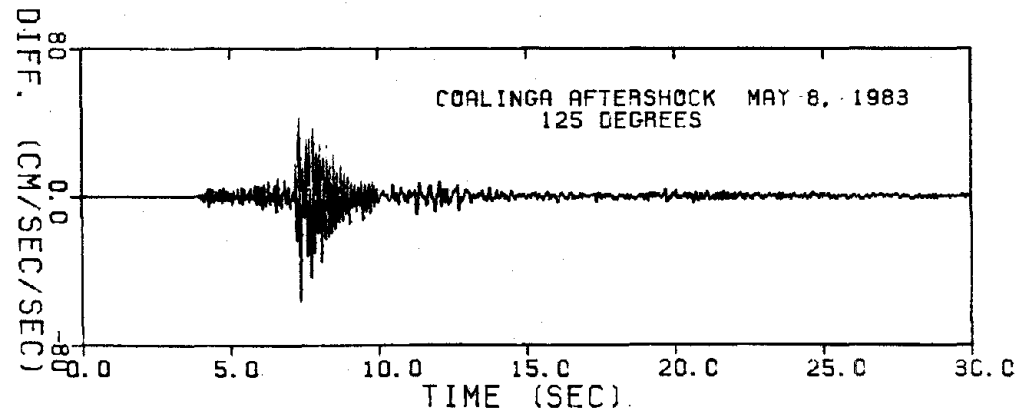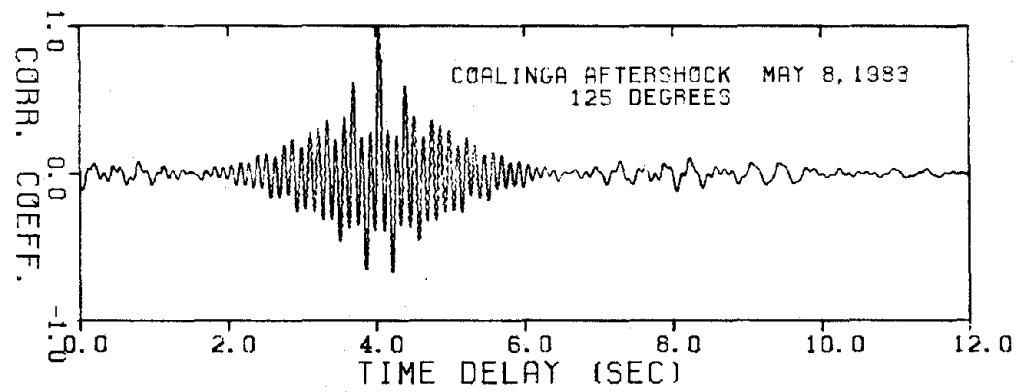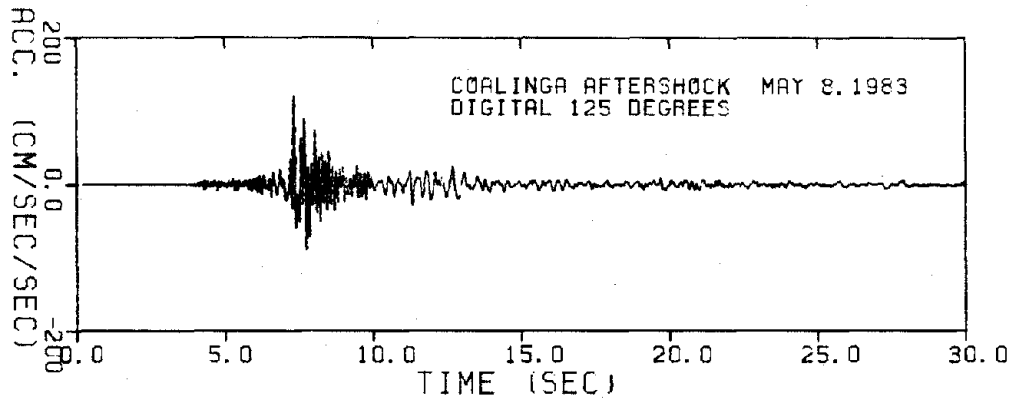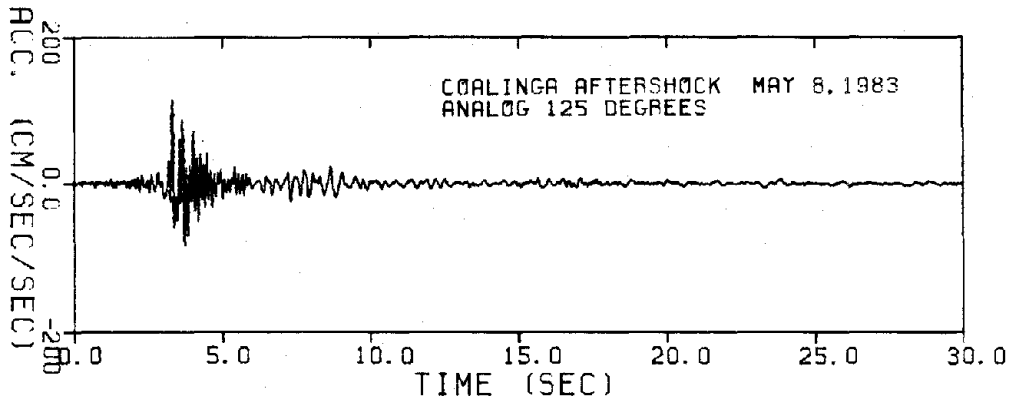
Figure 21 Correlation coefficient and difference between digital and analog
accelerograms. Coalinga aftershock, May 8, 1983; 125 degrees.
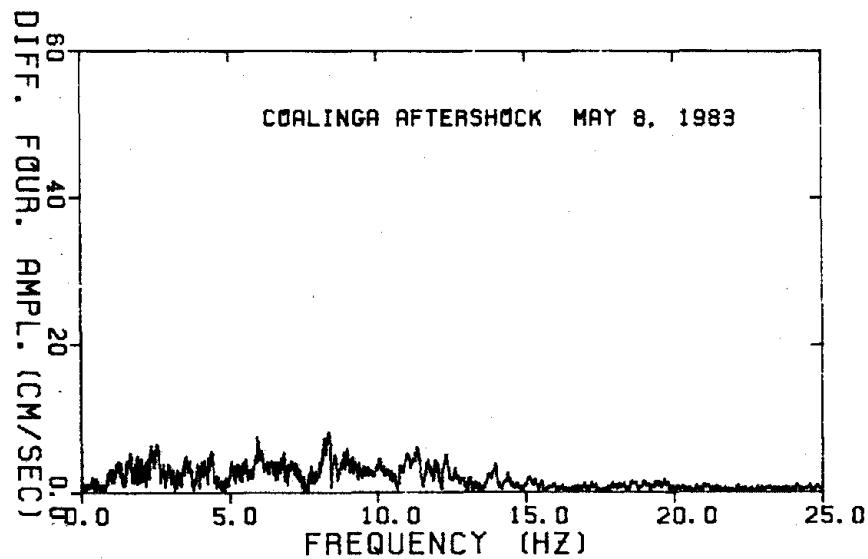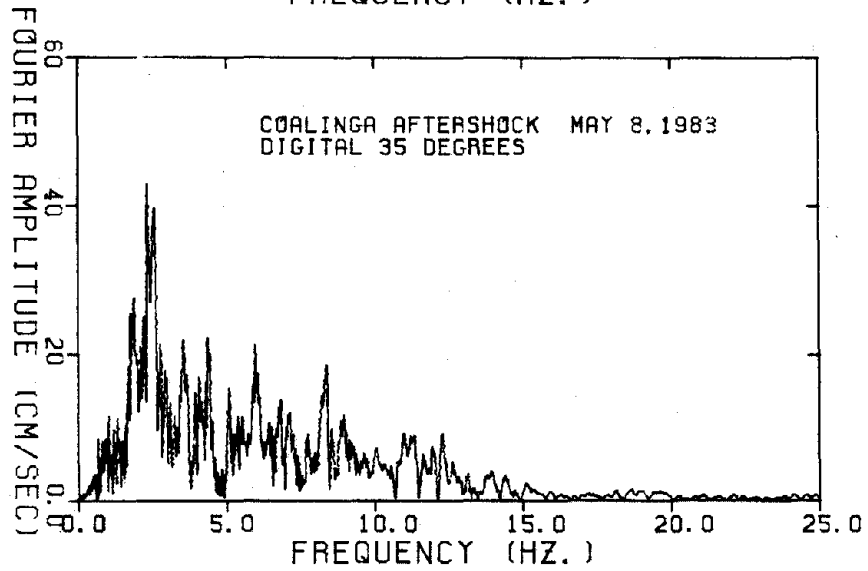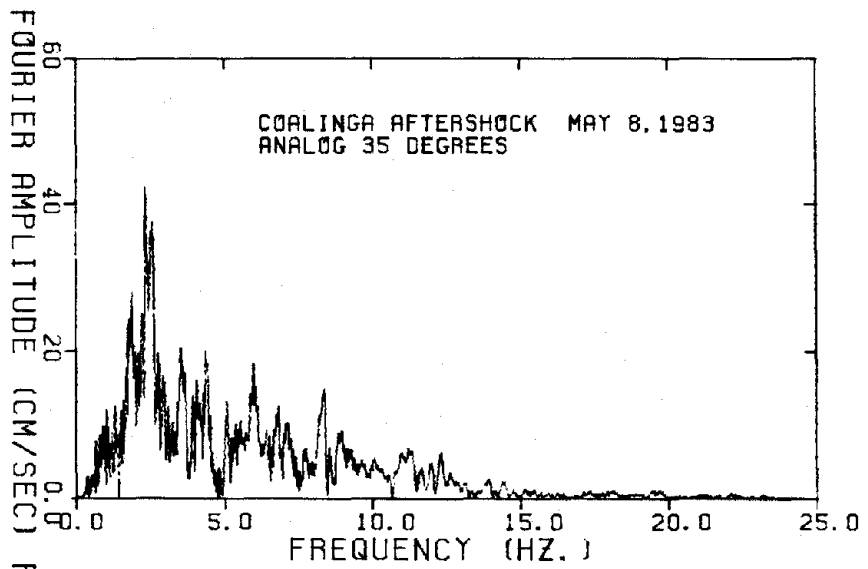
Figure 22 Fourier amplitude spectra of analog and digital accelerograms
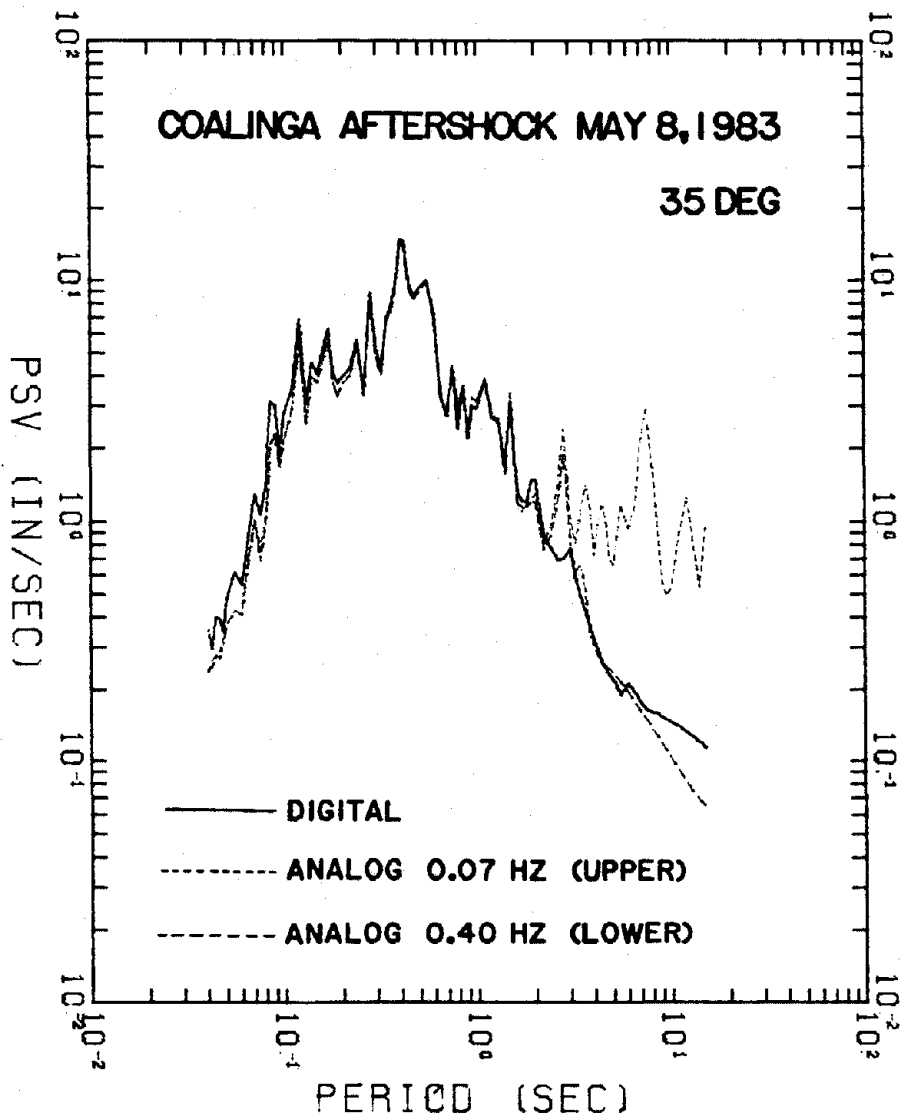and difference. Coalinga aftershock, May 8, 1983; 35 degrees.
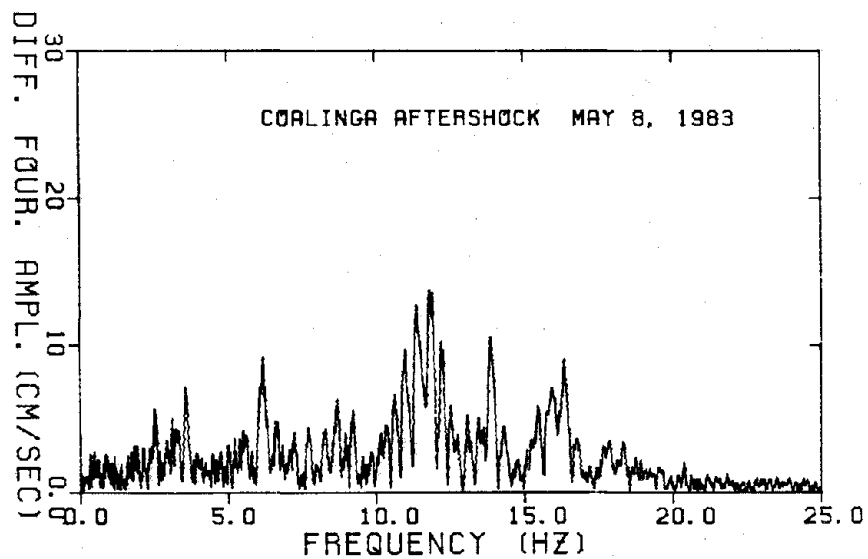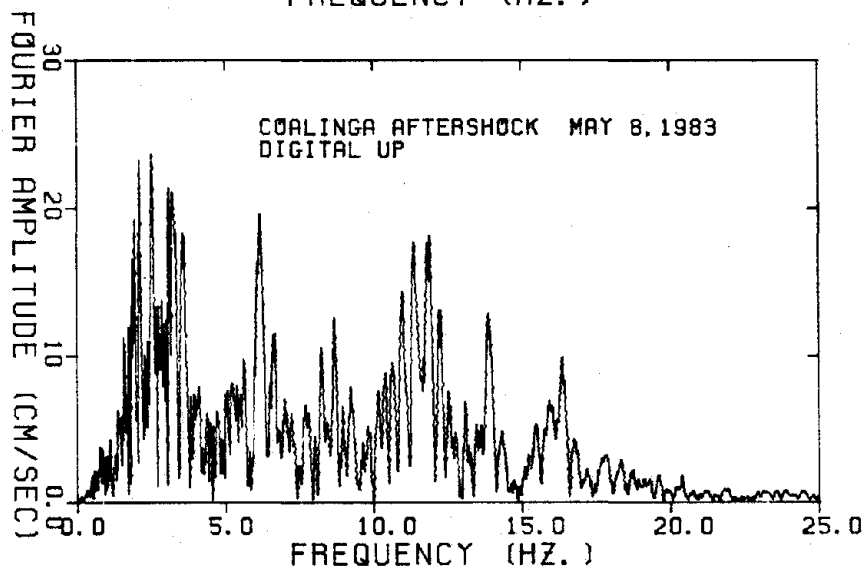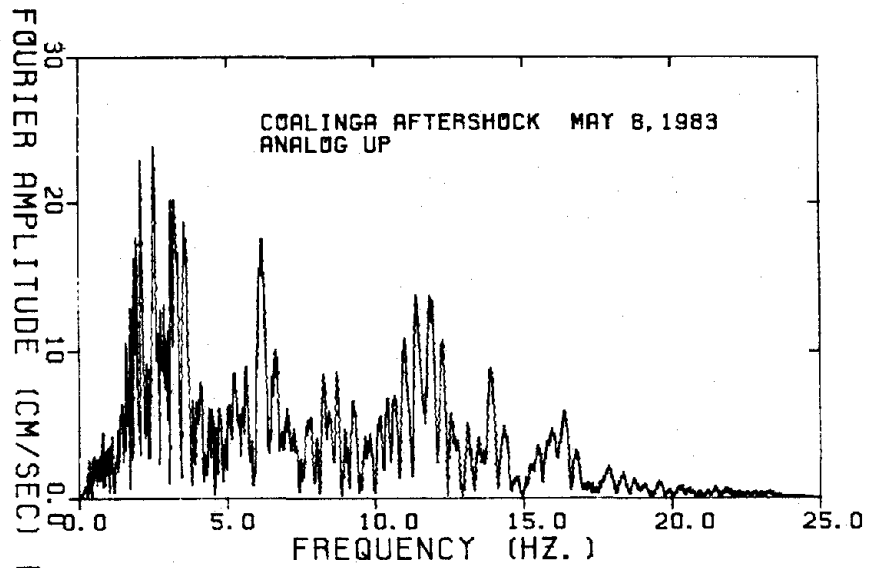
Figure 23 Fourier amplitude spectra of analog and digital accelerograms and
difference. Coalinga aftershock, May 8, 1983; up.
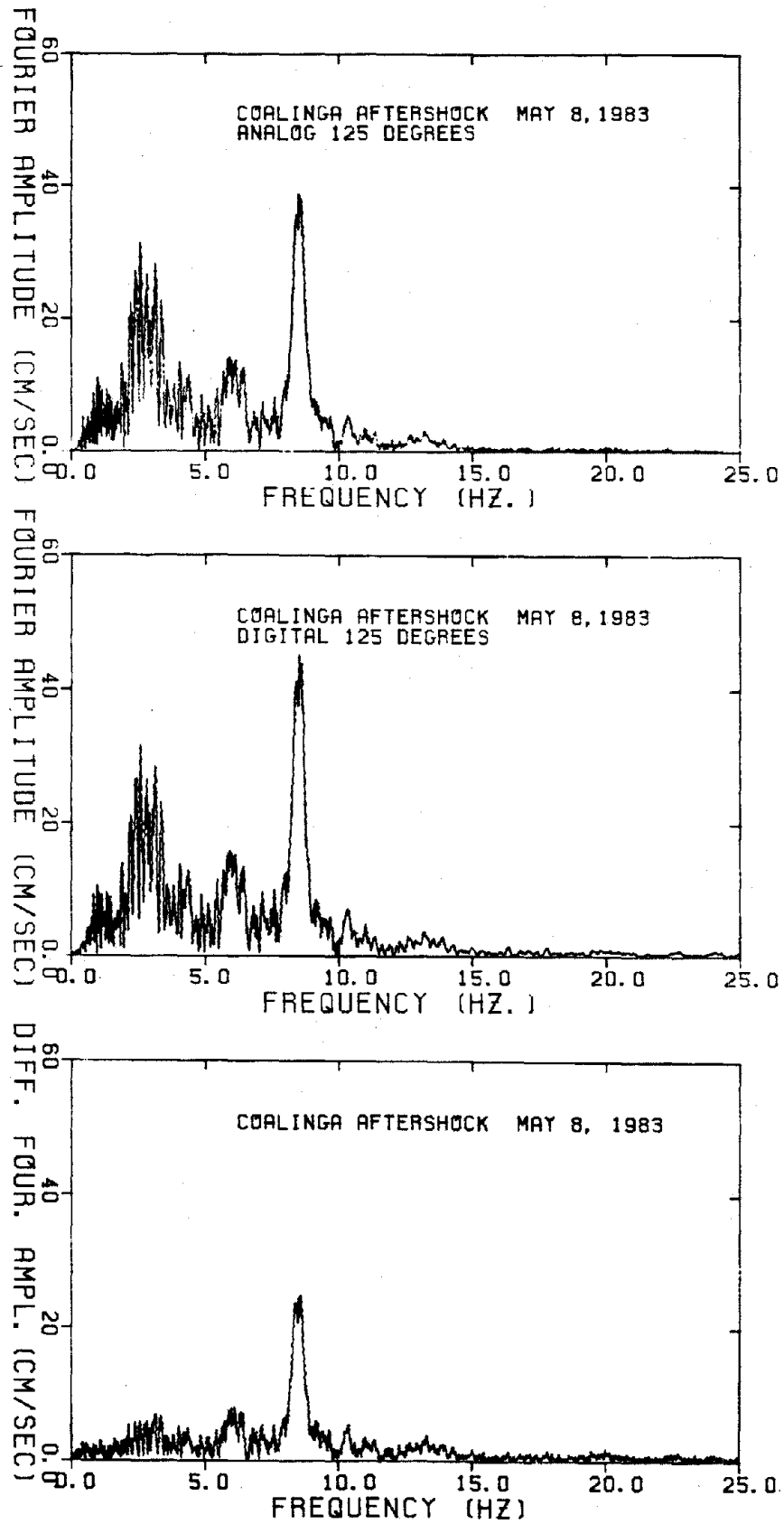
Figure 24   Fourier amplitude spectra of analog and digital accelerograms and difference.   Coalinga aftershock, May 8, 1983; 125 degrees.

Figure 25   Zero-damped response spectra of analog and
digital accelerograms. Coalinga aftershock,
May 8, 1983; 35 degrees.
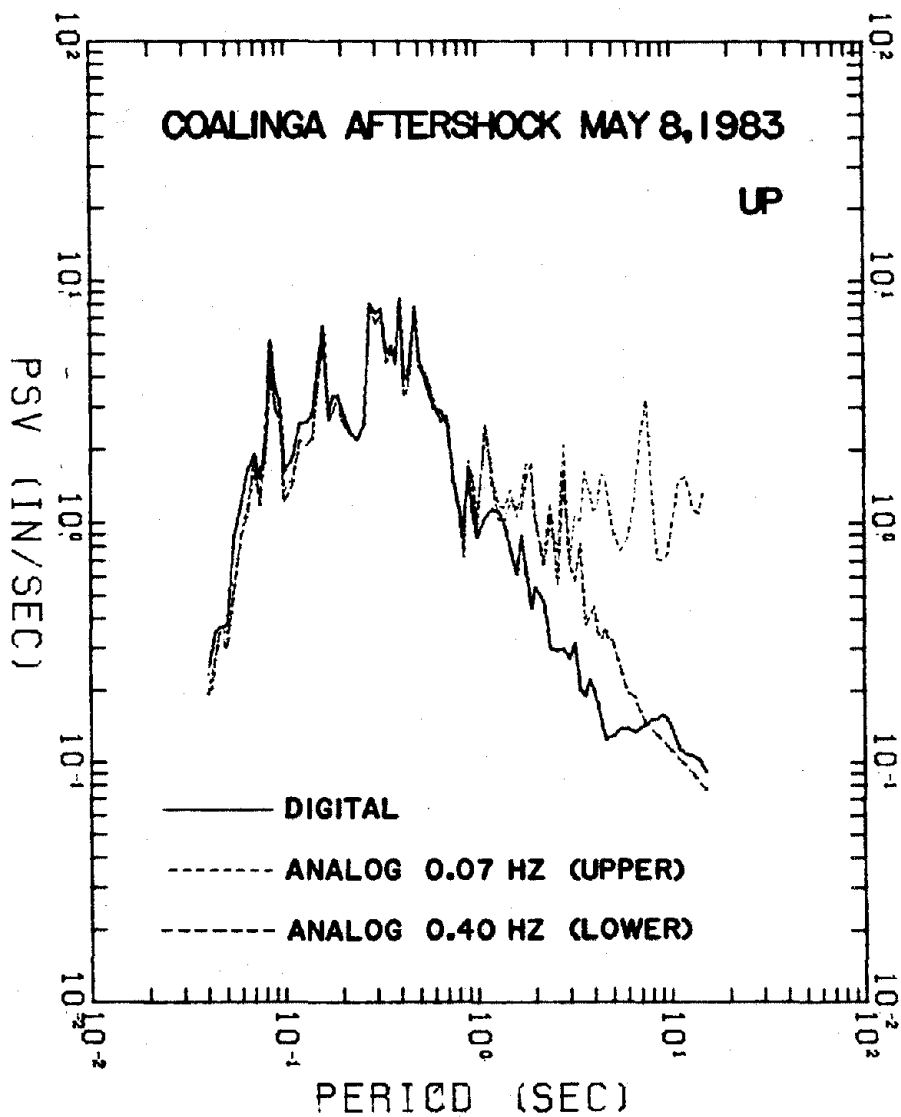
Figure 26   Zero-damped response spectra of analog and
            digital accelerograms. Coalinga aftershock,
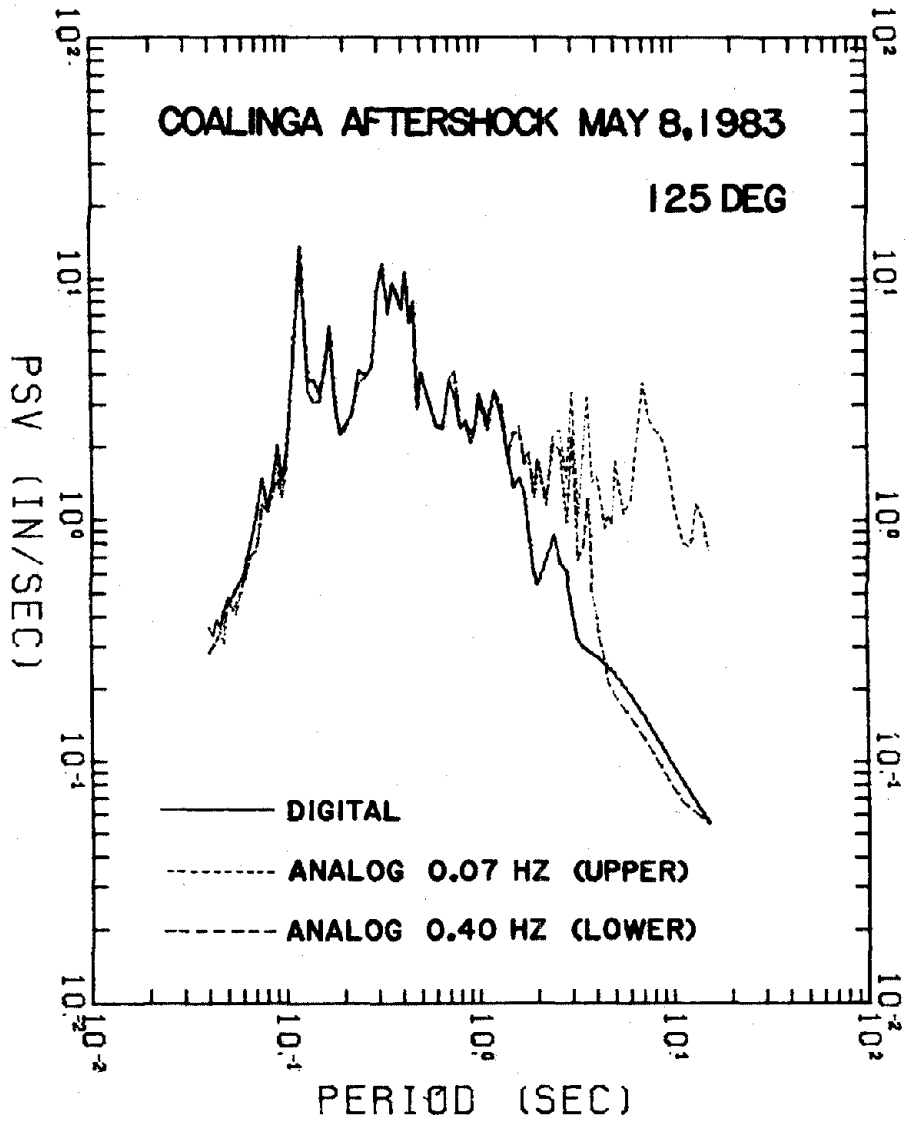   May 8, 1983; up.

Figure 27   Zero-damped response spectra of analog and
            digital accelerograms. Coalinga aftershock,
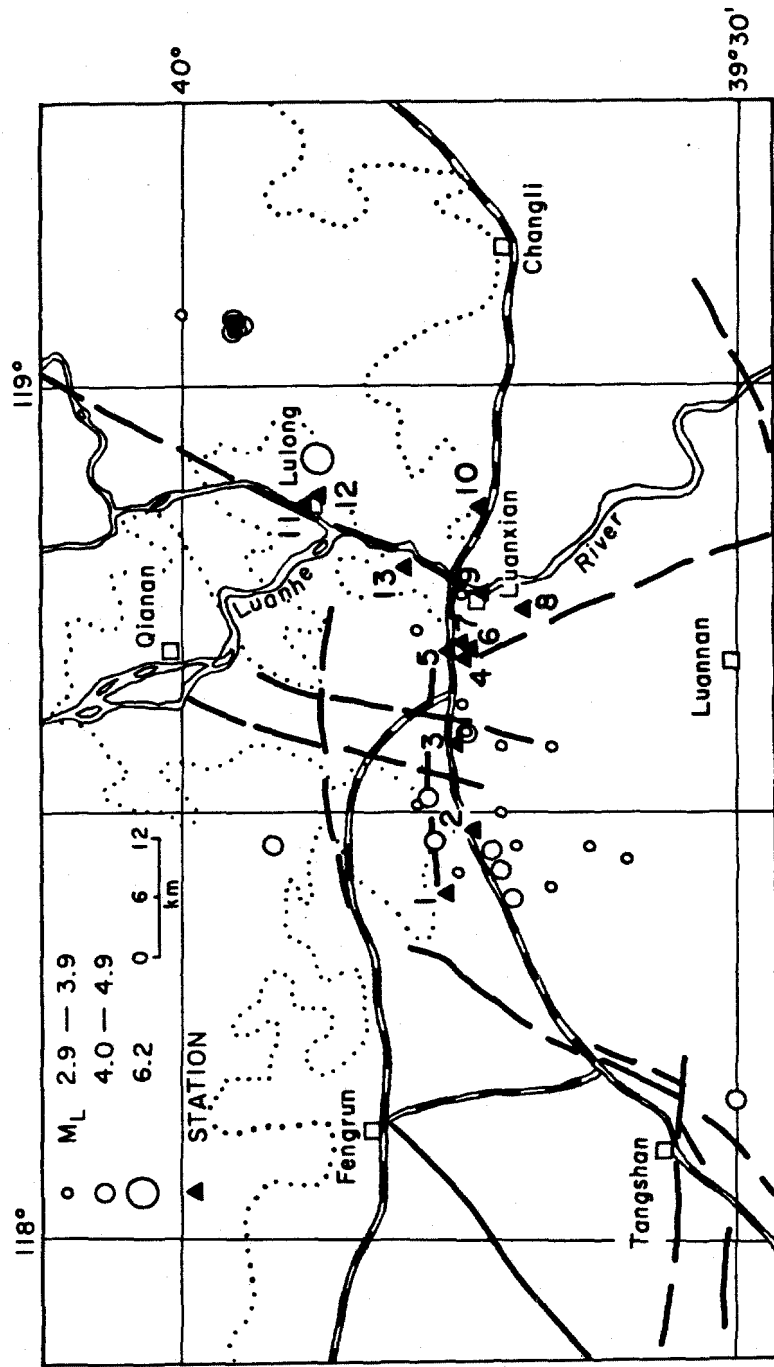   May 8, 1983; 125 degrees.

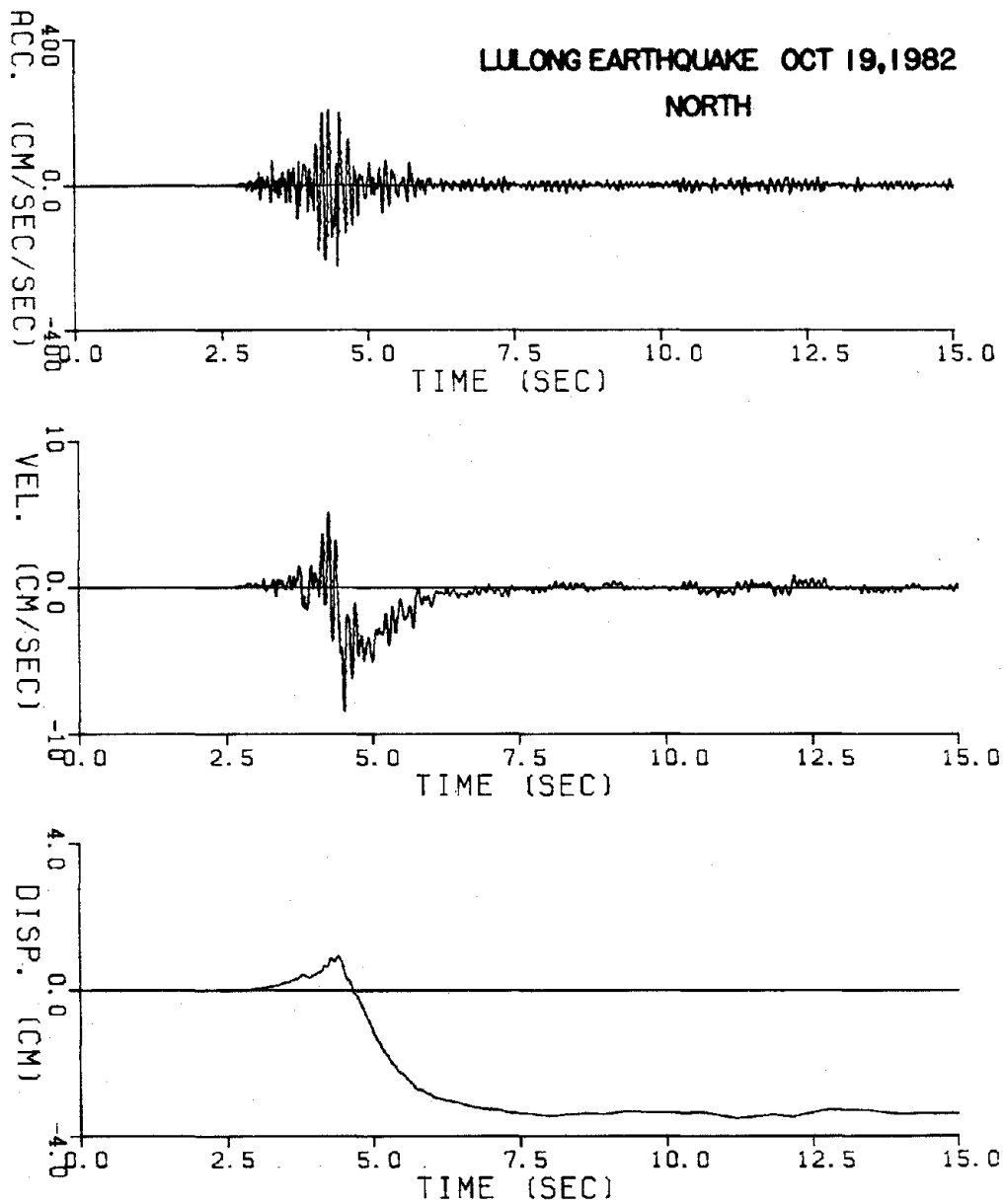Figure 28   Tangshan aftershock array showing location of Lulong event and
Station 11.

Figure 29 Accelerogram with integrated velocity and displace-
        ment. Station 12. Lulong earthquake, October 19, 1982;
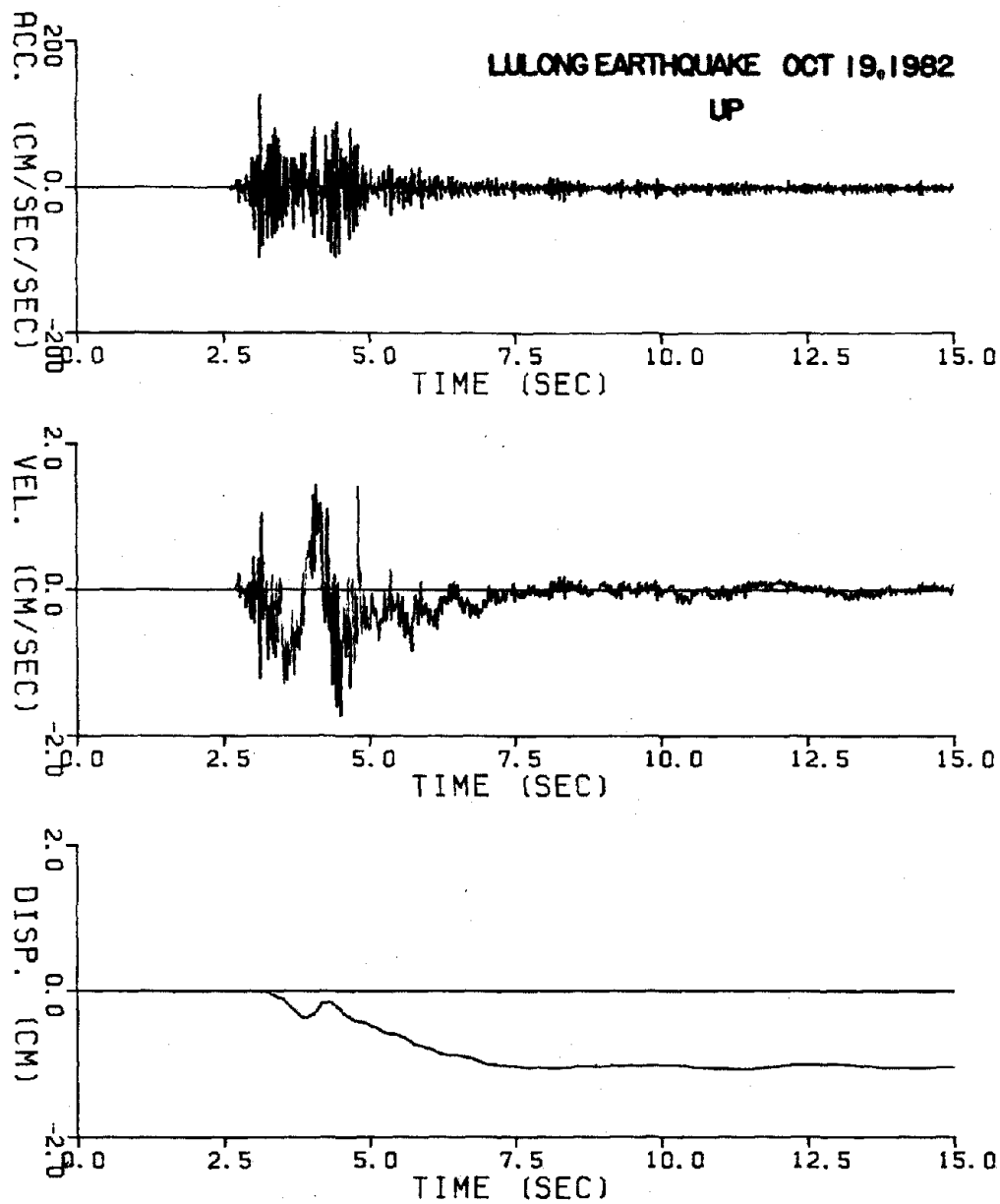   North.

Figure 30 Accelerogram with integrated velocity and displacement. Station 12. Lulong earthquake, October 19, 1982; up.
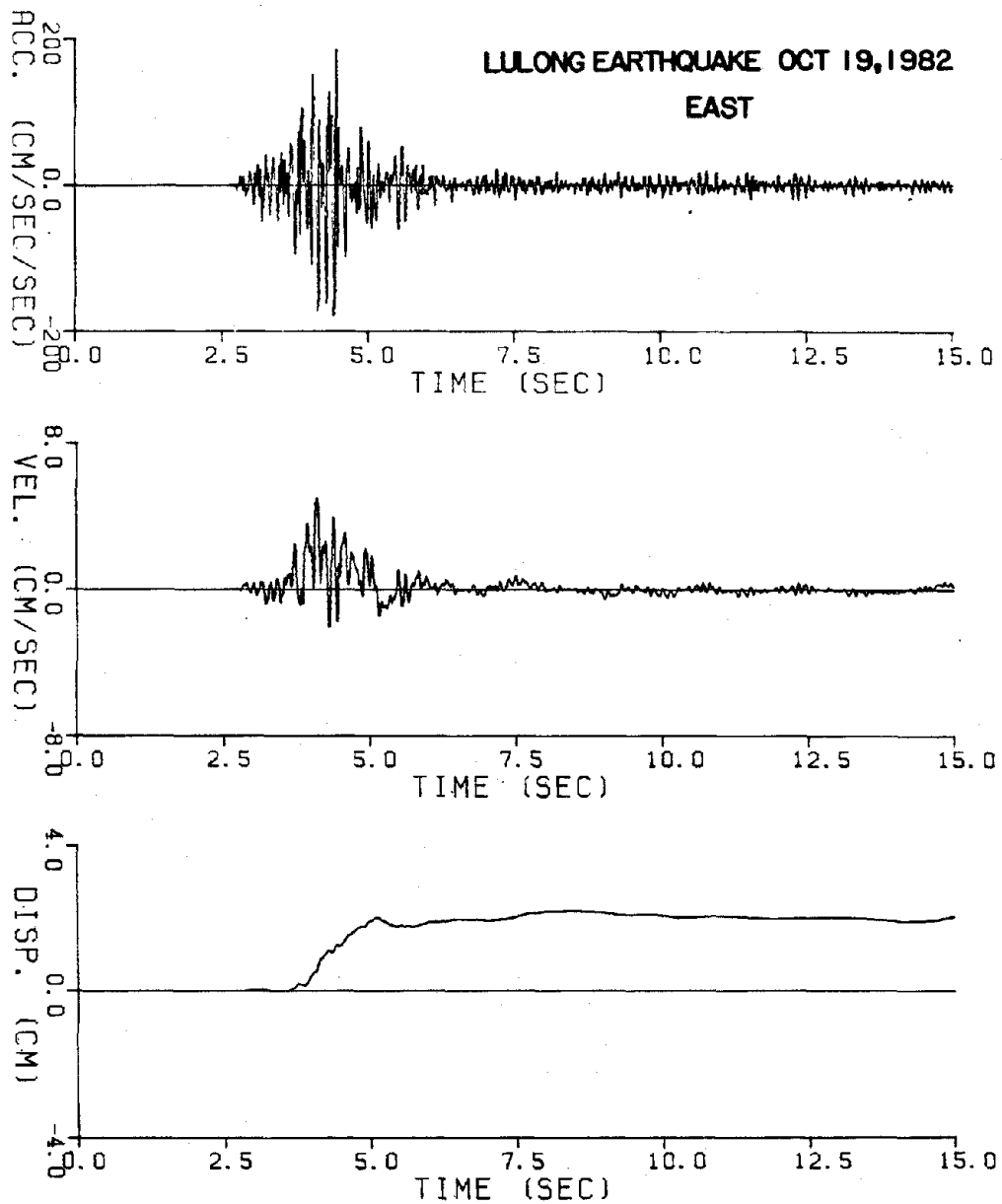
Figure 31   Accelerogram with integrated velocity and displace-
ment. Station 12. Lulong earthquake, October 19, 1982;
East.